REPORT DOCUMENTATION PAGE

AFRL-SR-BL-TR-99-

0347

1. AGENCY USE ONLY *(Leave blank)*	2. REPORT DATE	3. REPORT TYPE AND DATES COVERED
	December 1998	FINAL TECHNICAL REPORT 1 Jul 94-31 Dec 97

4. TITLE AND SUBTITLE
CONTROL OF FLOW IN COMPRESSORS BY SUCTION

5. FUNDING NUMBERS
F49620-94-1-0272

3484/WS

61103D

6. AUTHOR(S)
JACK L. KERREBROCK

7. PERFORMING ORGANIZATION NAME(S) AND ADDRESS(ES)
MASSACHUSETTS INSTITUTE OF TECHNOLOGY
77 MASSACHUSETTS AVENUE
CAMBRIDGE MA 02139

8. PERFORMING ORGANIZATION REPORT NUMBER

9. SPONSORING/MONITORING AGENCY NAME(S) AND ADDRESS(ES)
AIR FORCE OFFICE OF SCIENTIFIC RESEARCH
110 DUNCAN AVENUE SUITE B115
BOLLING AFB DC 20332-8050

10. SPONSORING/MONITORING AGENCY REPORT NUMBER

11. SUPPLEMENTARY NOTES

12a. DISTRIBUTION AVAILABILITY STATEMENT
APPROVED FOR PUBLIC RELEASE, DISTRIBUTION IS UNLIMITED

12b. DISTRIBUTION CODE

13. ABSTRACT *(Maximum 200 words)*
In this thesis, the design and construction of a low speed, aspirated fan   stage is described. The design intent of this stage is to increase the work   per blade row by control of the boundary layers within the flowpath. The low speed fan stage is designed to produce a pressure ratio of 1.5 at a tip speed of 700 fl/s. Any boundary layer that could limit the performance of the stage is controlled by suction at the location just upstream of the strong   deceleration of the free stream. The blade boundary layer was the primary   focus of the aspiration scheme, but the endwall boundary layers are also   treated. Implementation and design strategies for endwall and blade boundary layer removal are presented along with a description of the stage assembly andconstruction. Suction passages milled within the suction surface of the   blades in conjunction with cover plates provide a suction flowpath for blade boundary layer fluid removal through a tip shroud on the rotor. Endwall   boundary layer removal also plays a large part in the design of the complete aspirated stage. Slots are positioned just upstream of both the rotor and   stator tip shrouds for endwall boundary layer removal. The hub endwall   boundary layer is also suctioned immediately upstream of the stator.

14. SUBJECT TERMS

19991022 184

15. NUMBER OF PAGES
71

16. PRICE CODE

17. SECURITY CLASSIFICATION OF REPORT	18. SECURITY CLASSIFICATION OF THIS PAGE	19. SECURITY CLASSIFICATION OF ABSTRACT	20. LIMITATION OF ABSTRACT
U	U	U	

DTIC QUALITY INSPECTED 4

GAS TURBINE LABORATORY
DEPARTMENT OF AERONAUTICS AND ASTRONAUTICS
MASSACHUSETTS INSTITUTE OF TECHNOLOGY
CAMBRIDGE, MA 02139-4307

A Final Report on AFOSR Grant #F49620-94-1-0272

entitled

MECHANICAL DESIGN OF AN EXPERIMENTAL ASPIRATED COMPRESSOR

prepared for

AIR FORCE OFFICE OF SCIENTIFIC RESEARCH
801 N. Randolph Street
Arlington, Virginia 22203-1977

Attn: Lucinda R. Britt
Program Assistant

PRINICPAL
INVESTIGATOR: Jack L. Kerrebrock
                   Professor
                   Department of Aeronautics &
                       Astronautics

ASSERT Student: Brian J. Schuler

PERIOD OF
INVESTIGATATION: July 1, 1994 – December 31, 1997

December 1998

Mechanical Design of an Experimental Aspirated Compressor

by

Brian Joseph Schuler

Submitted to the Department of Aeronautics and Astronautics
on August 14, 1998, in partial fulfillment of the
requirements for the degree of
Master of Science of Aeronautics and Astronautics

Abstract

In this thesis, the design and construction of a low speed, aspirated fan stage is described. The design intent of this stage is to increase the work per blade row by control of the boundary layers within the flowpath. The low speed fan stage is designed to produce a pressure ratio of 1.5 at a tip speed of 700 ft/s. Any boundary layer that could limit the performance of the stage is controlled by suction at the location just upstream of the strong deceleration of the free stream. The blade boundary layer was the primary focus of the aspiration scheme, but the endwall boundary layers are also treated. Implementation and design strategies for endwall and blade boundary layer removal are presented along with a description of the stage assembly and construction. Suction passages milled within the suction surface of the blades in conjunction with cover plates provide a suction flowpath for blade boundary layer fluid removal through a tip shroud on the rotor. Endwall boundary layer removal also plays a large part in the design of the complete aspirated stage. Slots are positioned just upstream of both the rotor and stator tip shrouds for endwall boundary layer removal. The hub endwall boundary layer is also suctioned immediately upstream of the stator.

Thesis Supervisor: Jack L. Kerrebrock
Title: Professor of Aeronautics and Astronautics

Acknowledgments

Mark Drela and Ali Merchant provided invaluable insight and input into the design of the stage. Mark, in particular, for spending several hours with me writing a three dimensional spline tool. That is something that would have taken a couple weeks for me to do on my own. Like I heard someone else say, "I'm glad he's on our team." I'd like to thank Ali, in particular, for the rides to Turbocam and the ideas that you came up with in terms of the construction of the stage. Thanks also for the interesting conversation and company on the trip to Stockholm. I had a great time. I've learned so much over the past two years about design methods and thinking about all the details of an experiment that really make the difference between a good and bad experiment. Their insight will become even more valuable as the project proceeds into the experimental stage.

I would like to thank my parents, Greg, and Leigh for all their support over these past years. I've tried to live my life to the ideals which they so deeply instilled in me. I can trully contribute any success I have achieved to them because they made me who I am.

Thanks also to all the great guys (and gals) in the GTL. Thanks for dragging me out to play basketball or softball. Thanks to those who've moved on to bigger and better things, John, Brian, Eric, and Sonia, and those that will be soon, Ken and Allison, Jake. Thanks also to those brave souls that will be continuing on with me in the GTL, Margarita, Sanith, Rory, Dan, Chris, Jon, Kevin, and Adam. I hope to have many more sun-filled lunches with you on the steps of the student center. Thanks to Corinne for entertaining me while I was working on this thesis. Jean, Dennis, Luis, Shawn, and Malinda deserve a medal for putting up with my random visits, rant sessions, obsession with Canasta, and many other ways that I could annoy you. Thanks to you all for being such great friends. I'm a lucky guy.

The truth is I can't say enough about Prof. Jack Kerrebrock to express what he has meant to my development as a person not only in academia but in life as well. Ever since my freshman year when I got a UROP working on the Olympus hybrid rocket project which he was the advisor for, he has provided me with every great opportunity I can imagine. My two summers at NASA Lewis Research Center were a direct result of him, as well as my summer at AlliedSignal in Phoenix. My senior project was advised by him, and it was an amazing learning experience on how to design, build, and perform an experiment. It was during this process that I discovered how much I liked working in the lab. Finally, for the opportunity to work on this project that has such great potential and has already given me opportunities to meet people and see places that I otherwise would have never been able to see. All I can say is that I am humbled and honored to be working with him on this project. Thanks again for all your support and guidance. With him to rely on, the rest will only be better.

Finally, I would like to thank the person who is most important to me in my life. Thank you Judy for all those late night talks when I wasn't sure whether I was coming or going. Thanks for your cheerful smile and always excited demeanor. Sometimes I lose sight of what is important and you always pull me back to the right path. The long time and distance has made things tough sometimes, but you've always stuck with me, and I can't tell you how great that makes me feel. But soon we'll be closer and you might have to put up with me a little longer. Two down and two to go.

Contents

List of Figures

List of Tables

Chapter 1

Introduction

Increasing the stage pressure ratio has been an objective of compressor designers since the advent of the gas turbine. Most progress to this end has been made by increasing the blade speed of the compressor, because the work done per stage varies as the square of the wheel speed for similar flows. Structural considerations place an upper limit on the blade speed attainable so it is beneficial to explore other ways to increase work per stage. Boundary layer separation either on the endwalls or on the blade itself limits the performance of the blade row and causes increased losses. The central objective of aspirated compressors is therefore to control the boundary layer both on the blade and on the endwalls to increase the pressure rise per stage.

The concept of aspirated compressors was presented in Kerrebrock et al.[2] where the thermodynamic effects on engine performance were shown, and an experiment that explored the effects of boundary layer suction on the performance of transonic compressor blades was described. Removal of the viscous flow in a compressor system has two benefits on the performance of the compressor. Compressor efficiency can be increased by removal of the high entropy boundary layer fluid. Blade loading can also be increased by carefully placed boundary layer removal. By delaying separation, more turning can be done for a given blade speed.

If these performance objectives can be realized with a minimal amount of suction, weight savings and noise reduction can make the aspirated compressor an extremely attractive component in next generation engines. Weight savings are realized in the overall length of the engine. In modern commercial engines the fan and compressor comprise a large fraction of

the length of the engine. By doing more work per blade row, the total length of the compressor will decrease significantly and therefore the total weight of the engine would decrease. A decrease in fan noise is also a major benefit of aspirated compressors. Because of increased blade loading, the tip speed of the fan can decrease and still produce the same pressure ratio. With fan noise increasing as tip speed increases, aspirated fans can decrease fan noise.

1.1 Problem Statement and Motivation

The aspirated compressor is designed to control the blade and endwall boundary layers that normally limit the performance of a non-aspirated compressor stage. The aspirated compressor is designed to control all boundary layers that could limit the performance of the stage, so the first step is to understand how aspiration affects the flowfield.

Figure 1-1 compares calculated flows in a transonic cascade with and without boundary layer suction. The case on the left has suction applied just downstream of the shock on the suction surface of the blades while the other case does not have suction. Notice that the case without suction shows separation of the blade boundary layer immediately downstream of the shock. This separation causes large losses, decreased mass flow through the blade passage, and decreased turning. The case with suction shows a thin boundary layer all the way to the trailing edge. Its performance is characterized by lower losses, higher turning, and more pressure rise compared to the case without suction.

To be most effective, the position of the suction slot has to be properly chosen. Figure 1-2 shows the growth of a boundary layer under two limiting conditions, strongly attached flow and nearly separated flow. Its behavior can be determined from the von Karman integral momentum equation shown in equation 1.1. θ is the momentum thickness of the boundary layer, C_f is the skin friction coefficient, H is the shape factor, and u_e is the free stream velocity.

$$\frac{d\theta}{ds} = \frac{C_f}{2} - (2 + H)\frac{\theta}{u_e}\frac{du_e}{ds} \tag{1.1}$$

The downstream behavior of the boundary layer after a suction slot can be described by two limiting flow situations, as shown in figure 1-2. The $\triangle\theta_2$ originates from the suction flow. The two limiting cases are:

- **Strongly attached flow (Case A)**
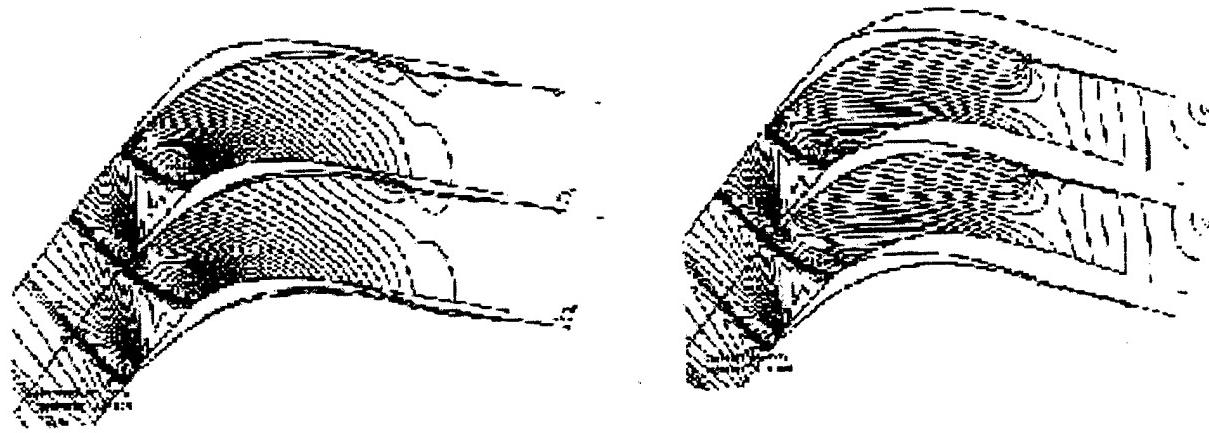
Figure 1-1: Comparison of Same Airfoil shown with and without Suction

$$\frac{d\theta}{ds} = \frac{C_f}{2}$$

$$\theta = \theta_2 + \int_{s_2}^{s} \frac{C_f}{2} ds \qquad (1.2)$$

$$\triangle\theta(s) = \triangle\theta_2$$

- **Nearly separated flow (Case B)**

$$\frac{d\theta}{ds} = -(2+H)\frac{\theta}{u_e}\frac{du_e}{ds}$$

$$\theta(s) = \theta_2 exp[\int_{s_2}^{s} -(2+H)\frac{1}{u_e}\frac{du_e}{ds} ds] \qquad (1.3)$$

$$\triangle\theta = \triangle\theta exp[\int_{s_2}^{s} -(2+H)\frac{1}{u_e}\frac{du_e}{ds} ds]$$

Strongly attached flow is characterized by a strong favorable pressure gradient and high skin friction, therefore the C_f term dominates the von Karman equation. In nearly separated flow, the boundary layer is passing through a strong adverse pressure gradient. The skin friction is nearly zero, therefore the $\frac{1}{u_e}(\frac{du_e}{ds})$ term dominates the equation.

13
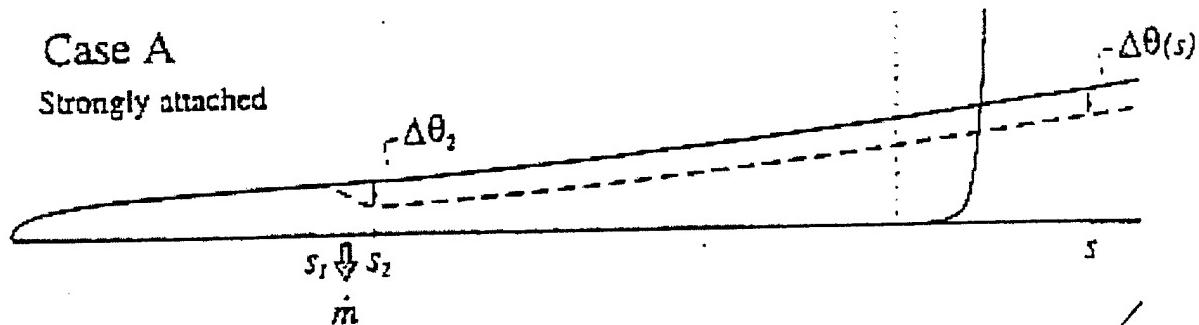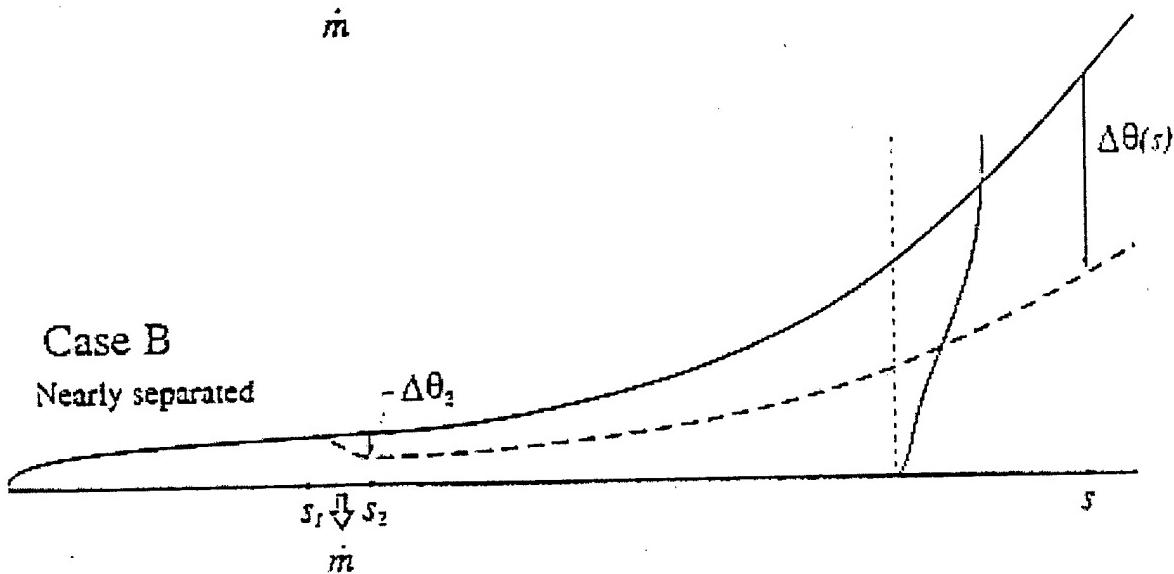
Figure 1-2: Effect of suction on boundary layer growth

Case A shows two boundary layer growth graphs. The solid line shows how the boundary layer would develop without the application of suction. From the points S_1 to S_2, suction is applied, causing a decrease in the momentum thickness of the boundary layer. The important point to note is that the difference in the two momentum thicknesses change little downstream of the suction slot. In Case B the difference in the two momentum thicknesses is magnified downstream of the suction slot by the exponential term shown in equation 1.3. Thus a small amount of suction can exert a large amount of control on the downstream boundary layer behavior in nearly separated flow regions.

For the greatest amount of control, suction should be applied just upstream of a large pressure recovery region, such as at a shock or on the aft portion of the suction surface of a blade. The exponential factor is greatest in these regions of flow, where $\frac{1}{u_e}(\frac{du_e}{ds})$ is quite

14

negative.

1.2 Background for Boundary Layer Suction

An exploratory experimental investigation into the concept of aspirated rotors was performed by Reijnen [5]. Five of twenty-three blades of an existing transonic rotor were modified for boundary layer suction. Suction scoops were added to the suction surface of the blade, positioned just downstream of the shock. The suction flow was taken radially inward, exhausting to a low pressure reservoir. The results of the experiment were that the blades with suction showed increased turning of the flow and a higher total pressure downstream corresponding to a higher efficiency. Another conclusion derived from the experiment was that to make full use of aspiration, the complete stage has to be designed with aspiration in mind. Adding aspiration to an existing stage will have only small performance gains.

In response to these results, Kerrebrock et al. [2] describe designs of low speed and high speed compressor stages. The low speed design produces PR=2 with $M_{tip} = 1.0$, and the high speed design produces PR=3 with $M_{tip} = 1.5$. These initial designs required large amounts of suction to keep the boundary layer from separating, as much as 4.9% for the low speed rotor and 8.7% for the low speed stator. The high speed design required as much as 14.4% for the rotor and 4.4% for the stator. A second generation of designs by Merchant et al. [1] was undertaken to improve the performance and reduce the bleed flow.

1.3 Family of Aspirated Compressors

Kerrebrock et al. [1] present this family of aspirated compressor designs that include two completed designs and one design in progress. The aerodynamics designs were performed by Ali Merchant using the MISES design tool modified for aspiration. Merchant [4] describes the solution process performed by MISES as well as the modifications that he made to the code to account for aspiration. Table 1.1 shows the important features of each of the designs.

For each design, the rotor tip and the stator hub were the most highly loaded sections making them the critical features of the stage. Figures 1-3 and 1-5 show the Mach number plots of the rotor tip and stator hub of the low speed compressor, and figures 1-4 and 1-6 show the pressure contours of the rotor tip and stator hub. For each section the suction slot is

15

Table 1.1: Aspirated Stage Design Features

	PR = 1.5	PR = 2.0	PR = 3.5
Tip Tang. Mach No.	0.70	1.00	1.5
Tip Speed (ft/s)	750	1000	1500
Axial Mach No.	0.65	0.67	0.68
Blade Row Suction Mass %	0.5	1.00	3.00
Max. Diffusion Factor	0.56	0.75	0.78
Rotor Tip Solidity	1.4	1.5	1.8
Stage Efficiency	0.94	0.92	0.87
Blade Loading, $\Delta H/U_{tip}^2$	0.86	0.72	0.61

placed just downstream of the shock. By taking off the boundary layer just downstream of the shock, much of the pressure recovery on the suction surface of the blade is done within a small fraction of the blade chord just downstream of the shock where the boundary layer is better able to handle the adverse pressure gradient. Then the pressure recovery farther downstream of suction can be tailored to keep the boundary layer attached all the way to the trailing edge.

1.4 Experimental Approach

The low speed design forms the basis for the experiment, the initial phases of which are the subject of this thesis. In particular, the thesis describes the mechanical design of the compressor stage for test in the MIT Blowdown Compressor facility. The removal of the blade boundary layer was the first concern of the project. For the initial design of the suction flow removal system, a systems point of view was taken, and the conclusion was that the boundary layer fluid would be removed through the tip of the blade. In this manner the rotor suction would be self-pumping and not require a secondary pumping system. In an engine application, the suction flow could simply be dumped overboard or used as cooling air in other parts of the engine. The suction flow would be transported to the tip of the blade through suction channels machined within the blade.

This thesis also presents schemes for removing the endwall boundary layer in locations where separation of the boundary layer may limit performance. In both the rotor and stator, the tip endwall boundary layers must pass through a passage shock. In order to minimize

R_TIP

MACH1 = 0.9470	MACH2 = 0.6426	
P1/P0 = 0.5614	P2/P0 = 0.7491	
SLOP1 = 1.0585	SLOP2 = 0.1221	
P2/P1 = 1.3345	RE = 2.260×10⁶	
ω = 0.0294	ωᵥ = 0.0151	
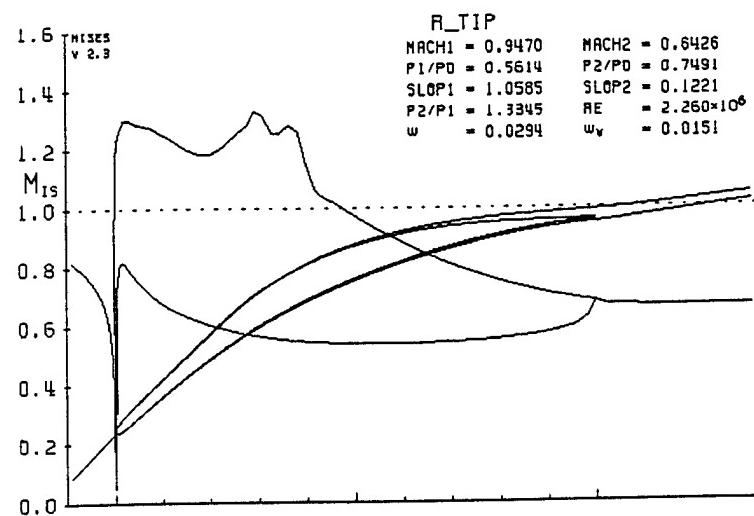
Figure 1-3: Surface Mach number plots for the rotor tip.

CONTOURS OF P/P₀
INCREMENT = 0.010
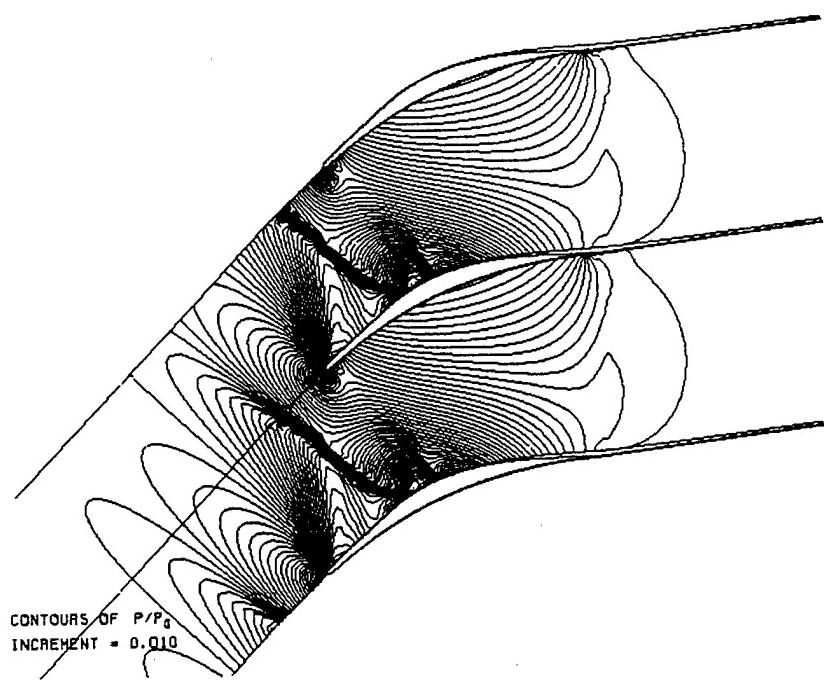
Figure 1-4: Pressure contours for the rotor tip.

S_HUB

MACH1 = 1.1300	MACH2 = 0.7176
P1/P0 = 0.4511	P2/P0 = 0.6764
SLOP1 = 1.3125	SLOP2 = 0.0198
P2/P1 = 1.4993	RE = 2.140×10^6
ω = 0.0852	ω_v = 0.0268
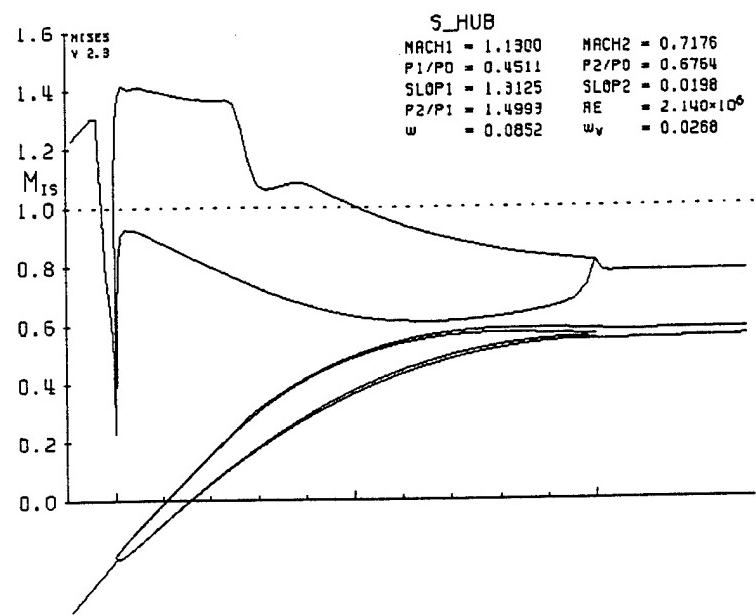
Figure 1-5: Surface Mach number plots for the stator hub.

CONTOURS OF PXR
INCREMENT = 0.010
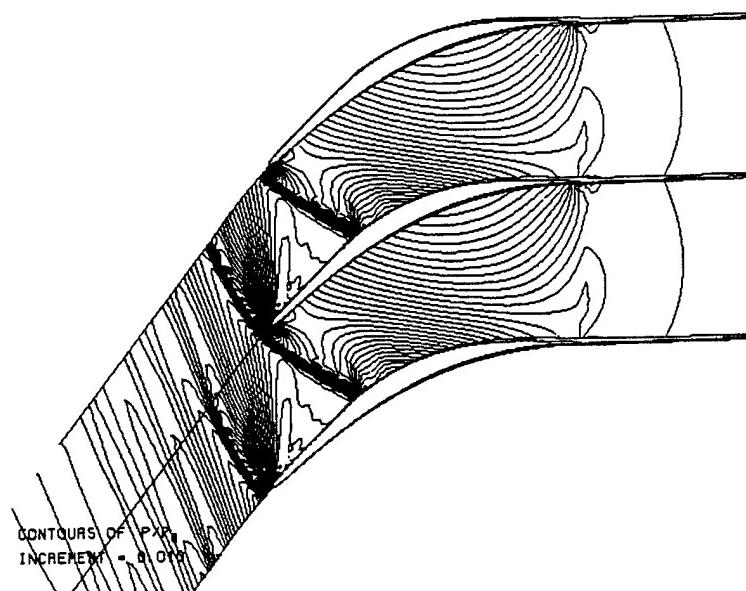
Figure 1-6: Pressure contours for the stator hub.

the possibility of separation, the endwall boundary layers are thinned out by suction just upstream of both blade rows.

1.4.1 Blade Boundary Layer Control

The goal of the aspirated compressor is to control the development of the boundary layer wherever it may hinder the performance of the compression process. The first limiting boundary layer that is addressed by the aspirated compressor is the blade boundary layer. Separation of the blade boundary layer in areas of high pressure gradient either on the blade suction surface or, in the case of transonic compressors, near the shock impingement point limits the turning, and hence amount of work, that a blade can do on the flow in a two dimensional sense. The separation creates a large recirculation zone that limits mass flow through the blade passage and limits how closely the flow can follow the blade suction surface.

The means for removal of the blade boundary layer fluid from the flowpath was addressed. Suction scoops were judged to be the best method of removing the flow for the reason that a portion of the dynamic head could be conserved by scooping the flow rather than bleeding the flow through slots in the blade.

Removal of the flow through the tip was determined to be the best method to deal with the suction flow for one reason. The reason was the increase in total pressure that the suction flow would receive from the centripetal acceleration of the rotor blades. Since the total pressure of the suction flow was increased from the free stream value, a separate pumping system is not necessary for the suction flow. This would decrease the complexity of the experiment and, for application in an engine, would eliminate the need for a separate pumping system. The suction flow could then simply be dumped overboard.

Removing the suction flow through the tip would require a tip shroud. The self-supporting tip shroud provides the blades with extra structural support and eliminates the tip clearance vortex normally formed by non-shrouded blade rows. Other required tip suction is also made easier by the addition of a tip shroud, including suction applied exactly at the shock impingement point on the shroud.

Implementation of the blade boundary layer suction requires removing the blade boundary layer from the flowpath and transporting it to the blade tip. The suction flow is transported to the tip via channels machined in the blades. To facilitate the manufacturing process, the

19

blades consist of two parts.

The first part is the original blade shape with radial channels milled out of the suction surface. The second part is a cover plate that fits over the suction channels to fill out the original suction surface. The cover plate contains a continuous slot that removes the blade boundary layer and deposits it into the blade suction channels. The centrifugal force of the rotating blades forces the suction flow to the tip where it is deposited overboard. Construction and attachment of the cover plates is discussed later in the thesis.

1.4.2 Endwall Boundary Layer

Having dealt with the suction surface boundary layer in a two-dimensional sense, the limitations imposed by the endwall boundary layers must be considered. The tip clearance flow is a major contributor to problems created by the endwall boundary layer. The integral shroud concept was introduced partly to deal with the tip clearance problem by eliminating the tip leakage flow. But the endwall boundary layers also behave poorly when passing through strong shock waves. The tip of the rotor and hub of the stator contain the strongest shocks. The tip of the stator contains a weaker shock, but the endwall boundary layer could separate as it passes through the shock. Therefore endwall suction is applied immediately upstream of the tip of the rotor, tip of the stator, and hub of the stator. The hub of the rotor does not contain a passage shock so it was decided that this is not a critical section of the stage.

Minimizing the size of the endwall boundary layer before it enters the stage is not enough. We must guarantee that the endwall boundary layer does not separate. To assure attachment throughout the stage, suction is applied at the passage shock impingement position on the tip shroud.

Within the rotor, the shock structure extends outwards from approximately 40% span to the tip and impinges on the shroud. The tip endwall boundary layer must pass through this shock surface. The adverse pressure gradient across the shock could cause the boundary layer to separate. To prevent this separation, suction is applied across approximately half the blade spacing downstream of the shock impingement location. The suction will keep the endwall boundary layer attached downstream of the shock. The same suction scheme is also applied at the tip of the stator.

1.4.3 Instrumentation

To determine the rotor and stator exit flow fields, the four-way probe provides complete data on the flowfield including total and static pressures, tangential angle, and radial angle. A detailed description of the four-way probe can be found in the doctoral thesis by Reijnen [5]. The four-way probe is used to measure the flowfield in the rotor-stator gap and downstream of the stator. With the use of a movable stator, the complete three-dimensional flowfield downstream of both the rotor and stator can be reconstructed.

Three high frequency Kulite wall pressure taps located upstream of the rotor determine the static pressure field and shock position in front of the rotor. Kulite wall pressure taps located in the blade passage on both the hub and shroud of the stator blade describe the pressure field and shock position within the blade passage.

To determine the suction mass flow of the stator, a Kulite pressure tap will be placed inside the suction channel and immediately outside the stator shroud. Kulite pressure taps will also be used to determine the amount of endwall suction being applied to the stage by measuring the pressure drop across the dump tank suction channels.

Low frequency pressure gauges provide information on the state of the facility. The pressures in both the supply and dump tanks are measured, and thermocouples located in the supply tank give measurements of the total temperature of the gas.

Chapter 2

Mechanical Design

The low speed aspirated compressor stage is to be tested in the MIT Blowdown Compressor. Figure 2-1 shows the general arrangement of the test system. The supply tank is pressurized with a mixture of carbon dioxide and argon. The mixture is such that $\gamma = 1.4$, but the molecular weight is more than air. With this mixture the speed of sound is approximately 80% of speed of sound in air. This lower speed of sound allows for a lower physical blade speed for the same blade mach number. Initially, the dump tank and test section are near vacuum and the supply tank is pressurized to approximately 80% of an atmosphere. For the test run, the rotor is spun up to speed in vacuum and then released from the motor. A valve releases the gas from the supply tank which flows through the test section to the dump tank. By matching the inertia of the rotor and the supply tank pressure, a constant tip mach number can be achieved over a test time of approximately 150 milliseconds. Kerrebrock et al. [3] designed, built, and tested the MIT Blowdown Compressor, and several validations have been performed using this testing method.

The mechanical design intent has the goal of transporting the fluid removed from the flowpath to the dump tank without interfering with the performance of the rotor or stator. For the blowdown compressor testing, the suction flow will be exhausted into the dump tank. The blowdown configuration allows for easy removal of the suction flow. Just like the main flow, the suction flow is also driven by the pressure drop between the supply tank and the dump tank. For the duration of the test time, the pressure in the supply tank is greater than 1.89 times the pressure in the dump tank. This means that all the suction flows are choked. By orificing the flows, the amount of suction flow can be metered.
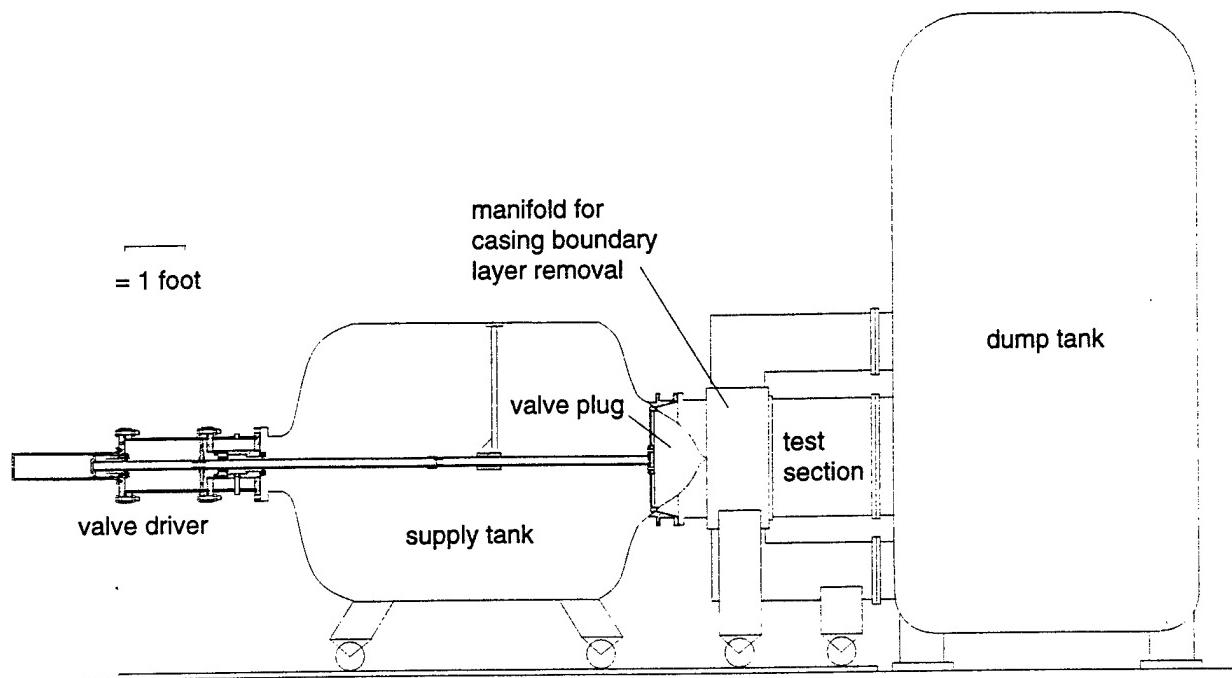
Figure 2-1: Schematic of MIT Blowdown Compressor

2.1 Integral Shroud

To eliminate diffusion limits imposed by tip leakage and to facilitate the transport of the suction flow from the blades to the dump channels, an integral shroud was adopted for the rotor. The rotor tip shroud and its seals form a plenum to carry the suction flow from the rotor. The plenum then empties the suction flow into the bleed flow channels which take the flow to the dump tank as shown in figure 2-2. Both the rotor and stator have integral shrouds.

An integral shroud design was adopted for both the rotor and stator for several reasons. Reijnen [5] drew the suction flow from the blade through the hub. To overcome the large pressure drop due to centripetal acceleration, the suction flow had to be removed by a separate vacuum tank. The tank introduced significant complexity in the experimental setup that could be eliminated with the addition of the integral shroud. With the shroud the blade suction flow could be taken out through the tip of the blade and dumped into the normal dump tank without adding an extra pumping system. The tip shroud is also more practical for implementation in an engine. The rotating channels increase the pressure of the suction flow

To Dump Tank

Suction Channels

Suction Slot
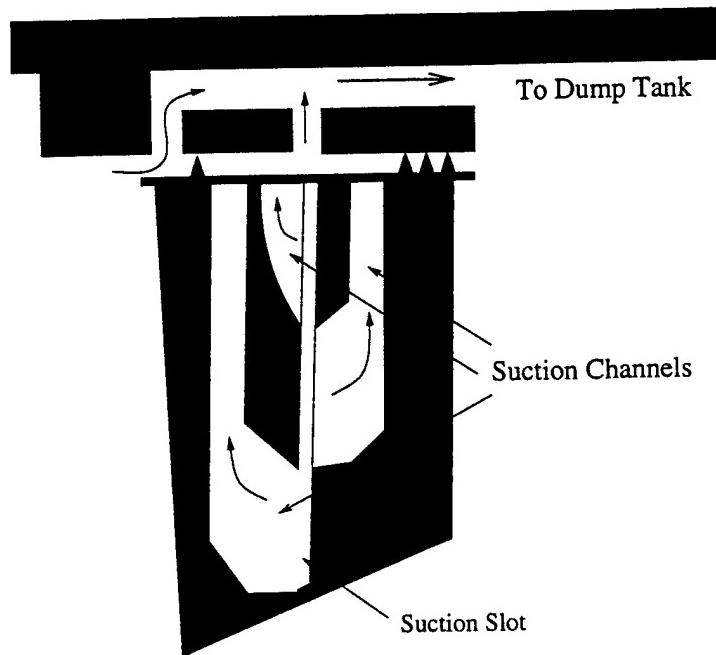
Figure 2-2: Schematic of Suction Flow Transport System

so that it can be exhausted immediately overboard. The tip shroud also eliminates the tip leakage flow and makes it easy to apply suction to other parts of the flow passage at the tip. This includes providing suction at the shock surface/casing boundary layer interface.

The integral shroud does provide a few problems as well. By taking the suction flow out of the tip, the fan rotor does work on that suction flow that is immediately lost when the suction flow is dumped overboard. This lost work is an inefficiency in the cycle. The tip shroud also provides problems with structural integrity of the rotor blades and disk. As the blade speed increases, the stresses in the shroud increase, and the material-limited stress in the system is reached at a much lower speed with a shroud than without a shroud.

In balance, the integral shroud design allows for a simpler experiment and accurately describes a practical design for an engine. The problems produced by the shroud are deemed much less significant than the benefits it provides. The efficiency loss due to taking the suction flow through the tip is small because the suction flow is small. A full structural analysis has shown that there are no serious structural problems at the blade speed used in the Blowdown

Compressor facility.

2.2 Bleed Flow Channels

The test section is set up with two casing pieces. The inner casing slides inside the outer casing. A set of parallel channels cut in the outer walls of the inner casing carry the suction flow from the main flowpath to the dump tank. The channels are sized to carry a much larger suction flow than is required. This oversizing reduces the speed of the flow within the channels also decreases the skin friction losses so as to make sure the main flow unchokes before the suction flow.

The channels are located within the casing of the test section. Three separate sets of channels carry different suction flows to the dump tank. One set carries the rotor casing suction exclusively. Another set carries the rotor blade suction and rotor shock/casing boundary layer interaction suction. The third set carries the stator blade suction, casing suction, and shock/casing boundary layer interaction suction.

2.3 Blade Suction Channels

The suction channels milled within the suction surface of both the rotor and stator blades carry the bleed air from the suction slot to the tip shroud of each blade. The suction channels are sized to carry three times the amount of suction used in the aerodynamic design without choking. The extra capacity will allow variations of suction strength to determine the best operating condition. The suction mass flow is controlled by radial choke holes that connect the blade suction channels to the outside of the tip shroud.

2.3.1 Rotor

In the rotor blades, the suction flow is self-pumping. The centrifugal force of the blades rotation drives the flow to the tip. At the tip, radial chokes holes in the shroud control the mass flow for the duration of the test.

The radial suction channels are sized to carry a maximum of three times the suction mass flow predicted by MISES. The extra capacity will allow for some variability within the testing scheme to do experiments comparing performance versus suction mass flow. In order to

determine the suction mass flow, the total pressure ahead of the choke holes must be known. To calculate the total pressure, the static pressure at the suction slot is determined from the MISES calculation. Then the total pressure at the tip of each section is calculated using a one-dimensional pipe flow code. Roughness and wall friction are approximated as well as the pressure rise gained by the rotation of the blades.

Figure 2-3 shows a three dimensional representation of the rotor blade without the cover plates. The suction channels divide the span of the blade into three sections with each channel flowing through its own choke holes. With the separate suction channels, the suction can be varied along the span. The feature is important due to the radial pressure gradient. If the suction was fed by a single slot, the radial pressure gradient would cause non-uniform suction along the span.
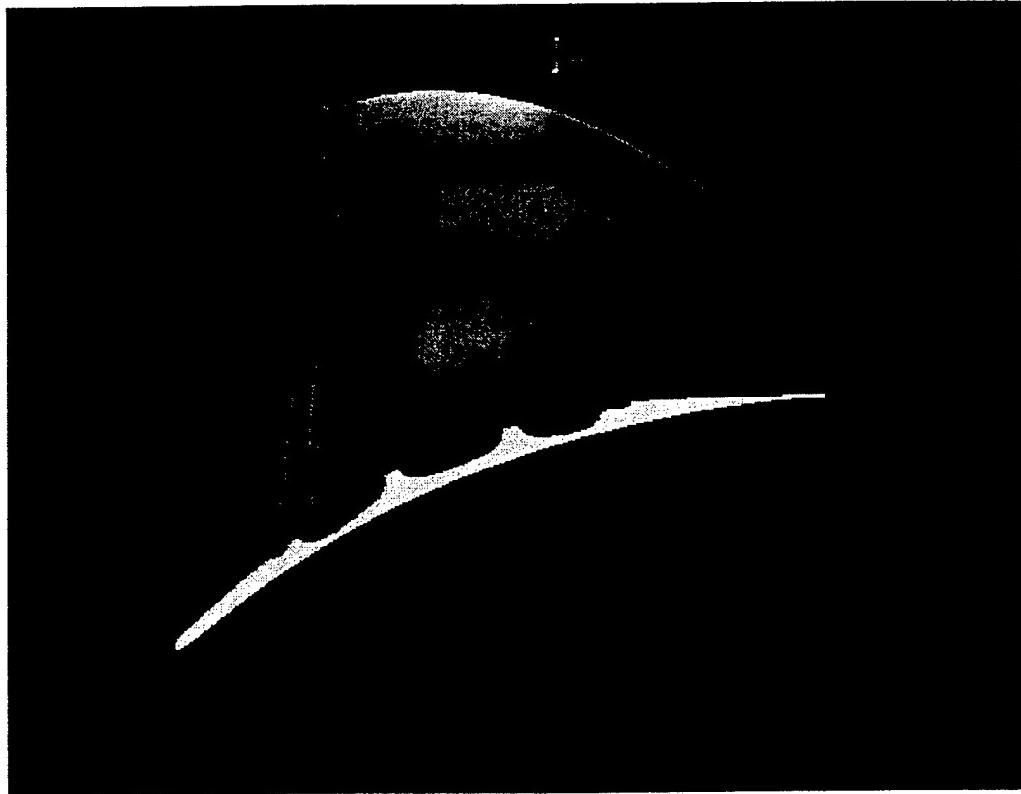

Figure 2-3: Three Dimensional Rotor Blade with Suction Channels

2.3.2 Stator

In the stator blades, the suction flow is driven by the pressure difference between the static pressure at the suction slot and the dump tank pressure. As in the rotor, radial choke holes in the shroud control the suction mass flow rate. The suction channel is sized to carry a maximum of three times the design suction mass flow.

Figure 2-4 shows a three dimensional representation of the stator blade without the cover plate. A single channel serves the entire span of the stator. Due to the smaller radial pressure gradient, a single channel is sufficient to create even suction along the span.

Figure 2-4: Three Dimensional Stator Blade with Suction Channels

2.4 Suction Slots

The blade suction slots are cut flush with the suction surface. The height of the boundary layer displacement thickness at the suction slot is only .006 inches. Therefore the inviscid streamlines will not be displaced by a significant amount by the mass removal. Figure 2-5

shows the suction scoop as it is implemented at the rotor tip.
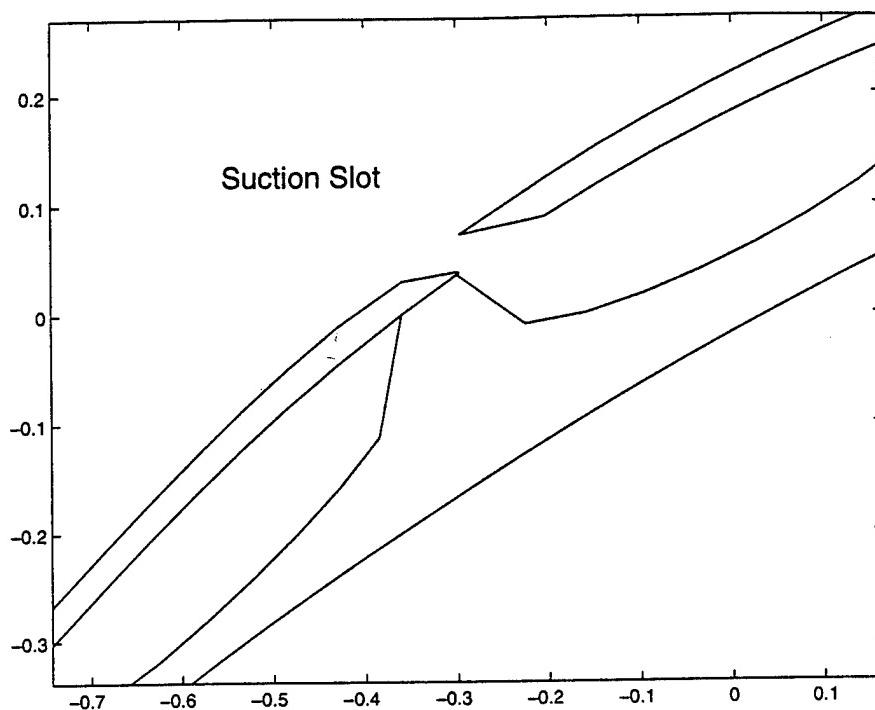
Figure 2-5: Close-up of Suction Slot Cross-section

2.5 Endwall Suction

Casing suction is applied immediately upstream of both the rotor and stator. This suction assures a clean, thin boundary layer entering the blade rows. A thin boundary layer is important to prevent endwall boundary layer separation as they pass through the passage shocks.

2.5.1 Rotor Tip Suction

The implementation of the casing boundary layer suction is shown in figure 2-6. A gap of .054 inch is shown between the rotor shroud and the casing piece that provides 1.29% suction of the through flow. This suction assures a clean endwall boundary layer entering the rotor. The rotor tip contains a strong passage shock. The design intent here is to not allow separation
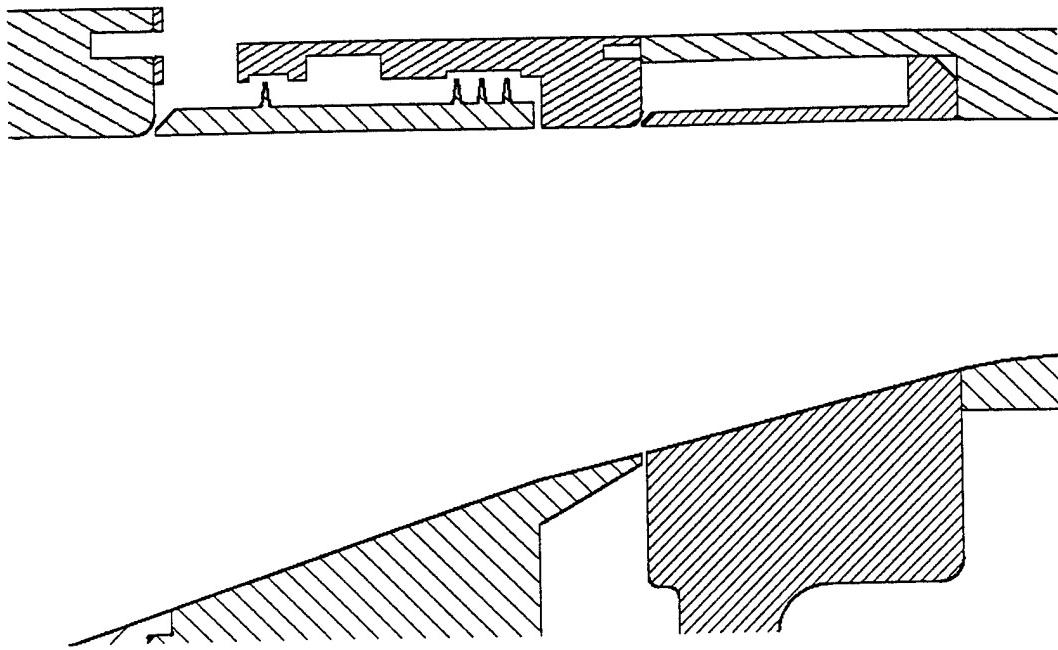
Figure 2-6: Casing Suction for Both Rotor and Stator

of an endwall boundary layer limit the performance of the stage. Therefore, the amount of suction is oversized so as to assure ourselves of a thin casing boundary layer.

2.5.2 Stator Tip Suction

The stator casing suction is implemented in a similar manner as the rotor casing suction and can also be seen in figure 2-6. A gap of .039 inch is shown between the rounded trailing edge of the casing and the sharp leading edge of the stator shroud. This provides 1.04% suction of the through flow.

2.5.3 Stator Hub Suction

The hub suction is applied immediately upstream of the stator hub section to assure clean boundary layer flow into the hub section of the stator. The stator hub has the highest diffusion throughout the entire stage so it is important to make sure that the hub boundary layer is well behaved. A gap of .062 inch is left between the end of the rotating spacer and the sharp

corner at the edge of the stator hub, and .50% of the through flow is suctioned.

2.6   Casing Shock/Boundary Layer Interaction Suction

In both the rotor and stator, the tip boundary layer must pass through a passage shock. To prevent separation of the boundary layer due to the shock, suction is applied through the integral shroud downstream of the shock. The amount of suction per unit length applied at this location is the same as the suction per unit length as that applied on the blade. The reasoning behind this is that the shock strength should be the same on the shroud as on the blade at the tip, and the boundary layer development is the same as on the tip section of the blade because the shroud boundary layer sees the same pressure field as the blade boundary layer.

2.6.1   Rotor

Figure 2-7 shows a view of the rotor shroud unwrapped in the tangential direction. The suction consists of eight suction holes staggered in the tangential direction. The holes extend 40% of the blade spacing beginning at the suction surface of one blade. The diameter of the holes are .125". The suction strength is .45% of the total mass flow.

2.6.2   Stator

Figure 2-8 shows a view of the stator shroud unwrapped in the tangential direction. The suction consists of eight suction holes staggered in the tangential direction. The holes extend 40% of the blade spacing beginning at the suction surface of one blade. The diameter of the holes are .065". The suction strength is .45% of the total mass flow.

2.7   Inlet Casing Contour

The contour of the inlet casing was designed to keep the casing boundary layer to a minimum as it developed upstream to the rotor. The contour was designed as an elliptical section to give an accelerating boundary layer all the way to the rotor face. This type of section will match the required slope conditions at both the inlet and the exit of the casing piece.

Shock Impingement Suction
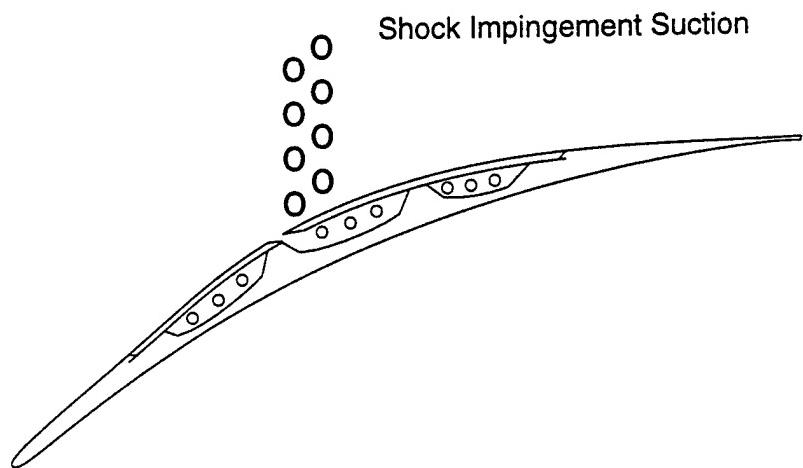
Figure 2-7: Rotor tip section

Shock Impingement Suction
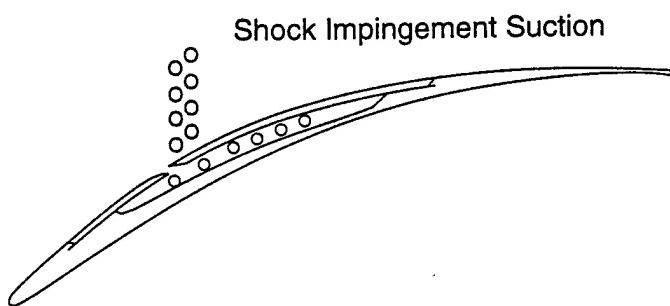
Figure 2-8: Stator tip section

32

2.8 Finite Element Structural Analysis

To insure the structural integrity of the integral rotor blade, shroud, and disk, a structural analysis was done using ANSYS and was performed by Dan Voron of AlliedSignal. ANSYS is a structural finite element method, and in this analysis, the shroud and disk were treated as axisymmetric models coupled with the blade. The blade stress analysis is done in the full three dimensions. The rotor blade is analyzed with the full geometry of the blade with suction channels that ran radially outward. The channels are not the exact channels to be used in the final experiment but capture the main structural features of the final blade. Three channels were made, one running the length of the channel, one running two thirds of the length, and the final one running only a third of the channel. The cover plates were not modeled in this analysis because they provide no structural support for the rotor. Appendix A contains the results of the ANSYS analysis. The shroud and disk are modeled as axisymmetric sections with the boundary conditions matching the interface with the 3-D blade analysis.

The ANSYS analysis showed the maximum stress within the rotor to be 35 ksi and localized to the trailing edge at the tip. This stress is lower than the 0.2% yield stress of 7075-Al of 58 ksi and is due to the mismatch of the radial extension realized by the shroud compared to the rotor trailing edge at this position. The shroud wants to expand more than the trailing edge which produces a local stress concentration. In practice, this part will be constructed with a fillet between the blade and the shroud. The fillet will decrease the stress in this region. This region was the only area that showed stresses close to the yield strength of aluminum.

Chapter 3

Construction and Data Collection

The important parts of the construction of the aspirated compressor stage involve attachment of the cover plates and an indexable stator. The casing sections, hub sections, spinner, supports, and choke plate are also in the construction of the stage. Figure 3-1 shows the assembly of the aspirated fan stage and includes all the parts that were designed for this stage. Appendix B contains the engineering drawings for each part. The assembly is fit around a bearing housing designed for tests in the Blowdown Compressor Facility. The bearing housing contains the bearings, shaft, and an oil seal for the rotor.

3.1 Cover Plates

The cover plates are technically the most challenging aspect of the aspirated stage. The complexity of the suction slot is contained within them. The cover plates themselves are stamped from $\frac{1}{32}''$ thick sheets of 2024-T6 aluminum. In order to limit the amount of spring back, the aluminum sheet is heated to a state where it is very malleable and has lost most of its strength. Then the sheet is formed into the shape of the suction surface by two steel stamps. As the sheet cools down, it gains some strength back and remains in the pressed shape. Since the cover plates are non-structural, the aluminum sheets do not need to have as much strength as the unheated sheets.

Then a five axis machine is used to created the suction slot. The initial cut of the slot is at approximately a 45 degree angle to the local slope on the surface of the plate. This cut creates a sharp leading edge for the downstream edge of the slot. The sharp leading edge is intended
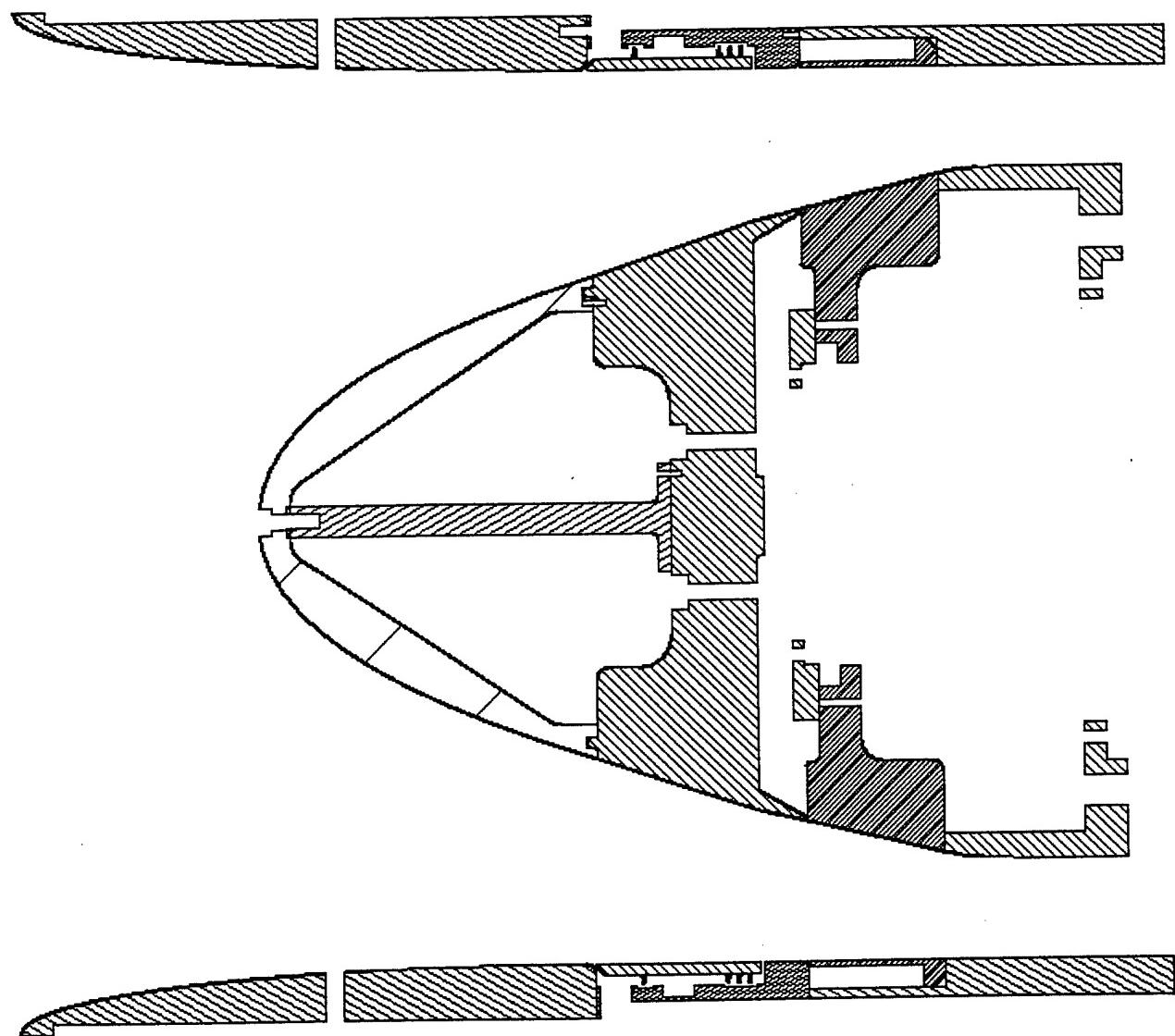
Figure 3-1: Cross-section of fan stage assembly

to prevent recirculation of suction flow back into the flowpath. Then surface of the plate just upstream of the slot is smoothed down to allow for a smooth flowpath for the boundary layer to follow from the suction surface to the suction slot.

The blades are machined with a recess for the cover plate. The recess lines up the cover plate and is deep enough to include the cover plate and .005″ of epoxy. The cover plate is attached to the blade with two methods. A strong epoxy is the primary bond between the cover plate and the blade. The cover plates are also held onto the blades with rivets at the four corners of the cover plate for support and to prevent peeling of the epoxy. In order to prevent cracking of the epoxy, the rivet holes must be drilled while the epoxy is curing.

3.2 Indexable Stator

An indexable stator is necessary for the aspirated compressor. The four-way probe can only take data at a single tangential location. Since the rotor spins during the test, data can be taken across the blade passage for each radial location, but since the stator doesn't move, the probe can only take data at one radial and one tangential location for each run. The probe easily moves in the radial direction but not in the tangential direction. Therefore, the stator was designed to be easily moved between test runs.

The stator was designed to be supported on a bearing that rests on the outside of the shaft bearing housing. A pair of bevel gears mounted to the outside of the test section are used to set the tangential position of the stator. The shaft of the gears go into the assembly radially and the teeth of the bevel gears attach to the teeth machined into the shroud of the stator. During a test run, the bevel gears are locked and hold the stator in place. The gears are mounted 180 degrees apart on the outside of the casing so that a pure moment can be applied to the stator when the tangential position is changed.

With the current design, the stator's tangential orientation can be changed for each run without having to take apart the complete assembly. This ability will save a lot of times between tests and allow data to be taken across the complete blade passage.

Chapter 4

Conclusions and Future Work

This thesis has presented a mechanical design that will enable experimental examination of the concept of Aspirated Compressors in the MIT Blowdown Compressor facility. Designs for implementation of boundary layer suction on the rotor and stator blades as well as endwall control have been presented. The design philosophy that has been used in this design is to control the boundary layer wherever it could limit the performance of the compressor.

4.1 Mechanical Design

In a two-dimensional sense, the blade boundary layer was the important limit to performance. The blade boundary layer flow was removed through slots located on the suction surface of the blade. After dealing with the blade boundary layer, separation of the endwall boundary layers had to be addressed. Suction that is applied at the critical locations just upstream of the rotor tip and stator hub thins out the boundary layer before it enters the blade row, and suction applied at the shock impingement locations prevent separation of the endwall boundary layer within the blade passage.

The construction and instrumentation for the aspirated compressor experiment is also described in this thesis. The construction of the cover plates is the most technically challenging aspect of the construction. Machining and attachment of the cover plates will be a time-consuming task. In terms of instrumentation and data collection, the four-way probe will provide the most meaningful information about the flowfield within the compressor stage, while other Kulite pressure transducers provide information about the shock structure in

front of the rotor and within the stator.

4.2 Experiment and Future Work

This master's thesis has presented the design and construction of a low speed compressor stage that takes advantage of aspiration to produce a high work, high efficiency stage based on the work by Merchant [1]. The testing of this stage and subsequent analysis of the data from the tests is the continuation of this masters thesis and will become the bulk of my doctoral thesis. This experiment will be the first test of aspiration on a complete compressor stage and will comprise the major portion of my doctoral thesis. The experimental aspirated stage is designed to deliver PR=1.5 for $M_{tip} = 0.7$ at 94% stage efficiency. The experiment will be considered successful if the performance of the stage is as predicted with an acceptable suction flow rate. Tables 4.2 and 4.2 show the breakdown of the predicted suction for both the rotor and stator. For the experiment, a total suction of 4.73% is predicted for the stage.

Blade Suction	0.50%
Casing Suction	1.29%
Shock/Boundary Layer Suction	0.45%
Total Suction	2.24%

Table 4.1: Rotor Suction Requirements

Blade Suction	0.50%
Casing Suction	1.04%
Hub Suction	0.50%
Shock/Boundary Layer Suction	0.45%
Total Suction	2.49%

Table 4.2: Stator Suction Requirements

The experimental schedule is to determine the design point performance maps and compare that to the computational results. The experiment will also determine the off-design operation of the stage, including whether more suction will be required to achieve the necessary operating range that is required for implementation in an engine. Optimization of the suction flows for both the design point and for off-design operation is a large part of the

upcoming experiment. Adjustment of the blade suction rate and the endwall suction rate in the experiment will determine the exact nature that the suction has on the compressor stage. Therefore it is important that the design presented in this thesis allows for easy adjustment of the suction flows.

Future work consists primarily of conducting the experiment as the design has described as well as analysis of the results. No impediments that could prevent realization of this objective have been identified, and construction of the experiment has proceeded. Construction of the main components of the experiment including the casing and hub pieces, rotor blisk, and integral stator blades and disk is currently under way. Construction of the cover plates is scheduled to begin shortly.

Appendix A

Ansys Stress Analysis of Low Speed Aspirated Compressor

This appendix contains the results of the stress analysis performed on the low speed aspirated compressor. The Ansys finite element package was used for the calculations. For the analysis, an axisymetric two-dimensional model was used for the shroud and disk while a fully three-dimensional model was used for the blade. Ansys resolves both the stresses and strains in the axial, radial, and tangential directions.

The main results of the stress analysis were that the strains produced by the low speeds were within the tolerances of the machining capability therefore no modifications of the blade geometry were needed before fabrication. The calculated stresses were also much lower than the yield stress of aluminum. The high stress region of the blade at the tip near the trailing edge. The radial strain of the shroud causes the blade to stretch more than it normally would. With a relatively thin trailing edge, the stress concentration is greatest in this area. The stress in this region is still lower than the yield stress of aluminum, and the analysis did not take into account the fillet between the blade and shroud. This fillet will provide some stress relief.

MIT ASPIRATOR
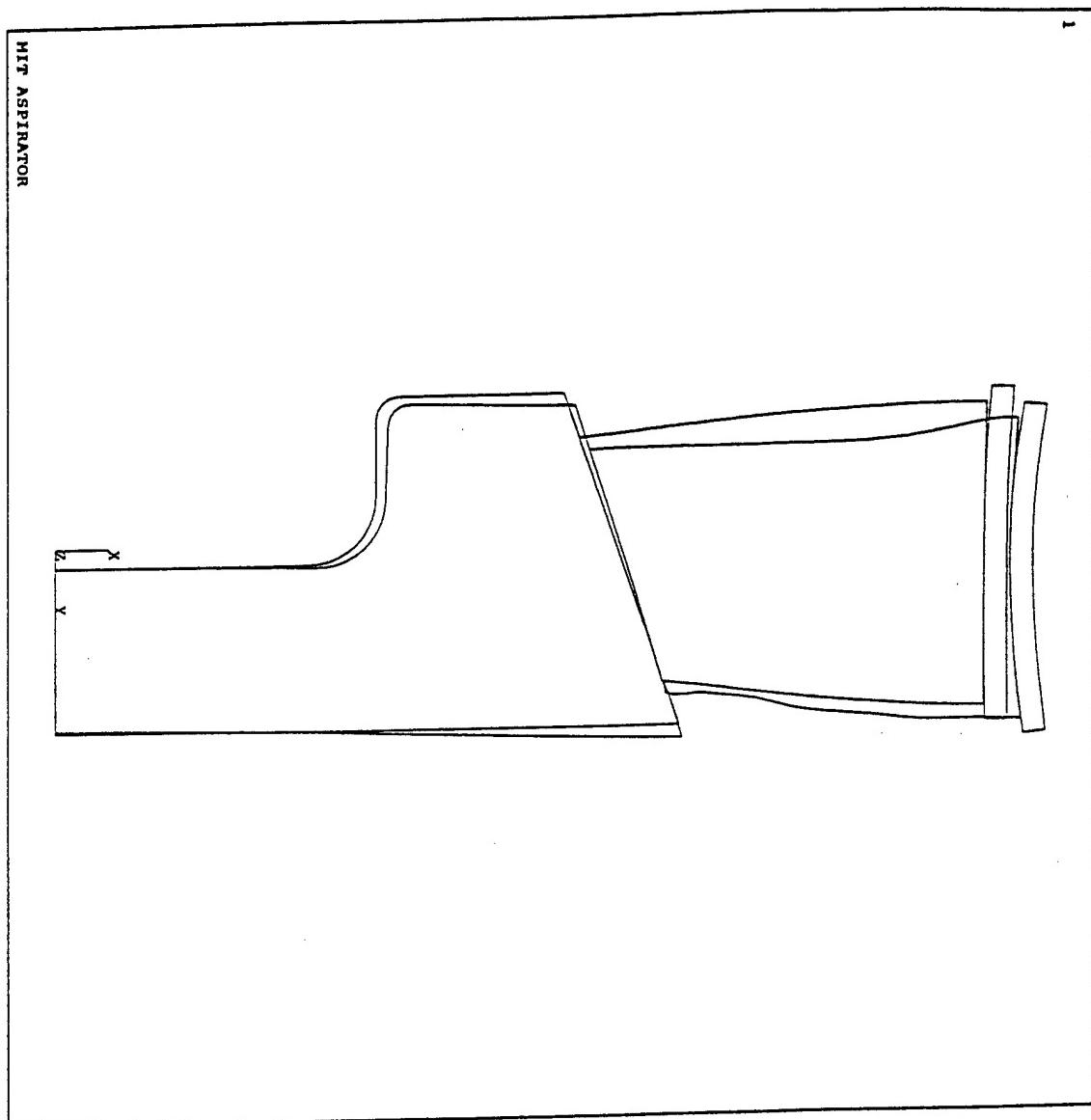
ANSYS 5.3
MAR 30 1998
11:13:45
PLOT NO.   1
DISPLACEMENT
STEP=1
SUB =1
TIME=1
RSYS=11
DMX =.007805
SEPC=27.912

DSCA=67.268
ZV =-1
DIST=5.974
XF =5.431
YF =.337582
ZF =-.25002
VUP =X
PRECISE HIDDEN
EDGE

Figure A-1: Exaggerated Displacement Plot
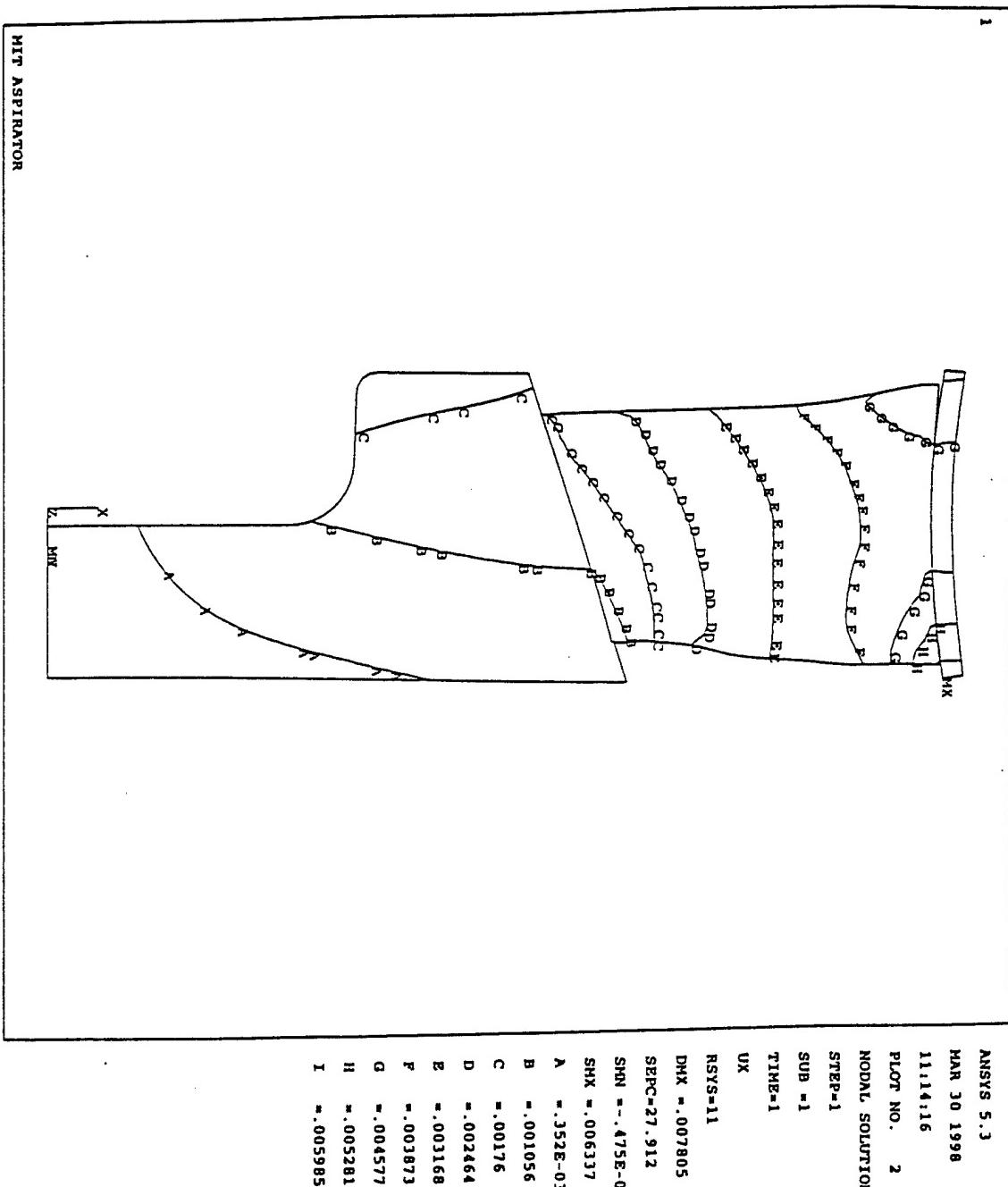
Figure A-2: Radial Deflection (in)

HIT ASPIRATOR

ANSYS 5.3
MAR 30 1998
11:14:39
PLOT NO.   3
NODAL SOLUTION
STEP=1
SUB =1
TIME=1
UY
RSYS=11
DMX =.007805
SEPC=27.912
SMN =-.002686
SMX =-.004463
A =-.002289
B =-.001495
C =-.700E-03
D =.940E-04
E =.888E-03
F =.001683
G =.002477
H =.003271
I =.004066
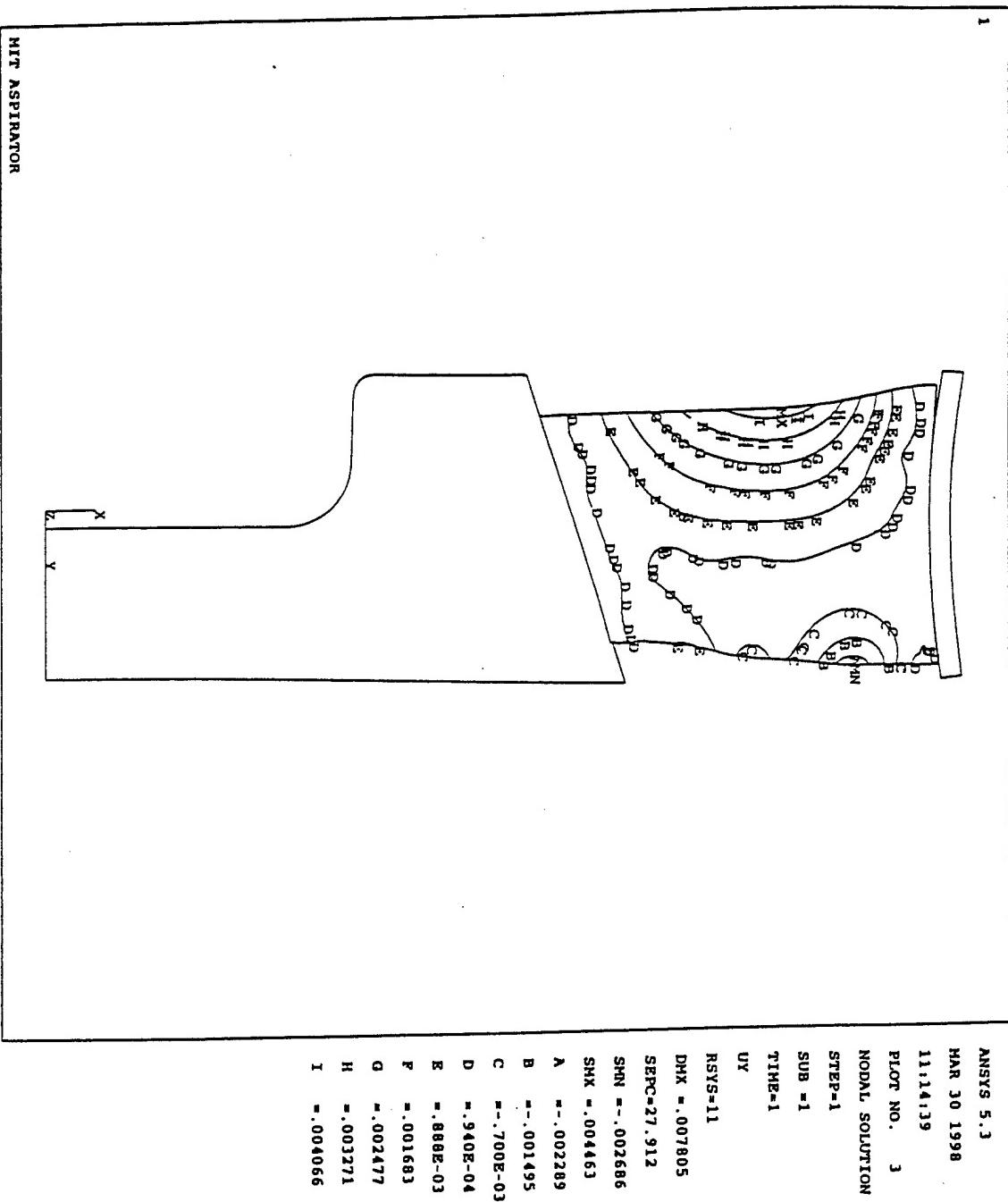
Figure A-3: Tangential Deflection (in)

46

Figure A-4: Axial Deflection (in)
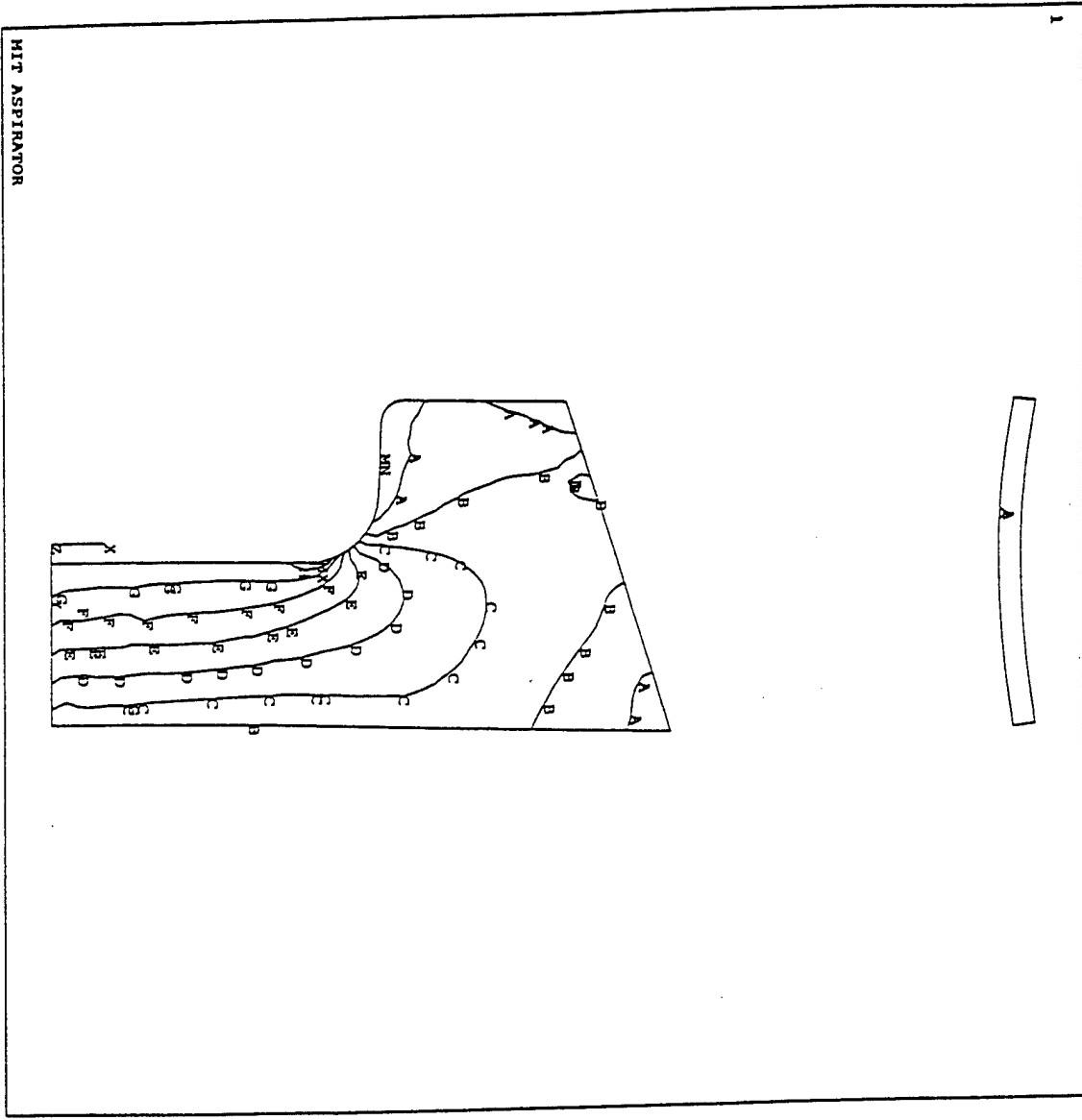
Figure A-5: Radial Stress (psi)
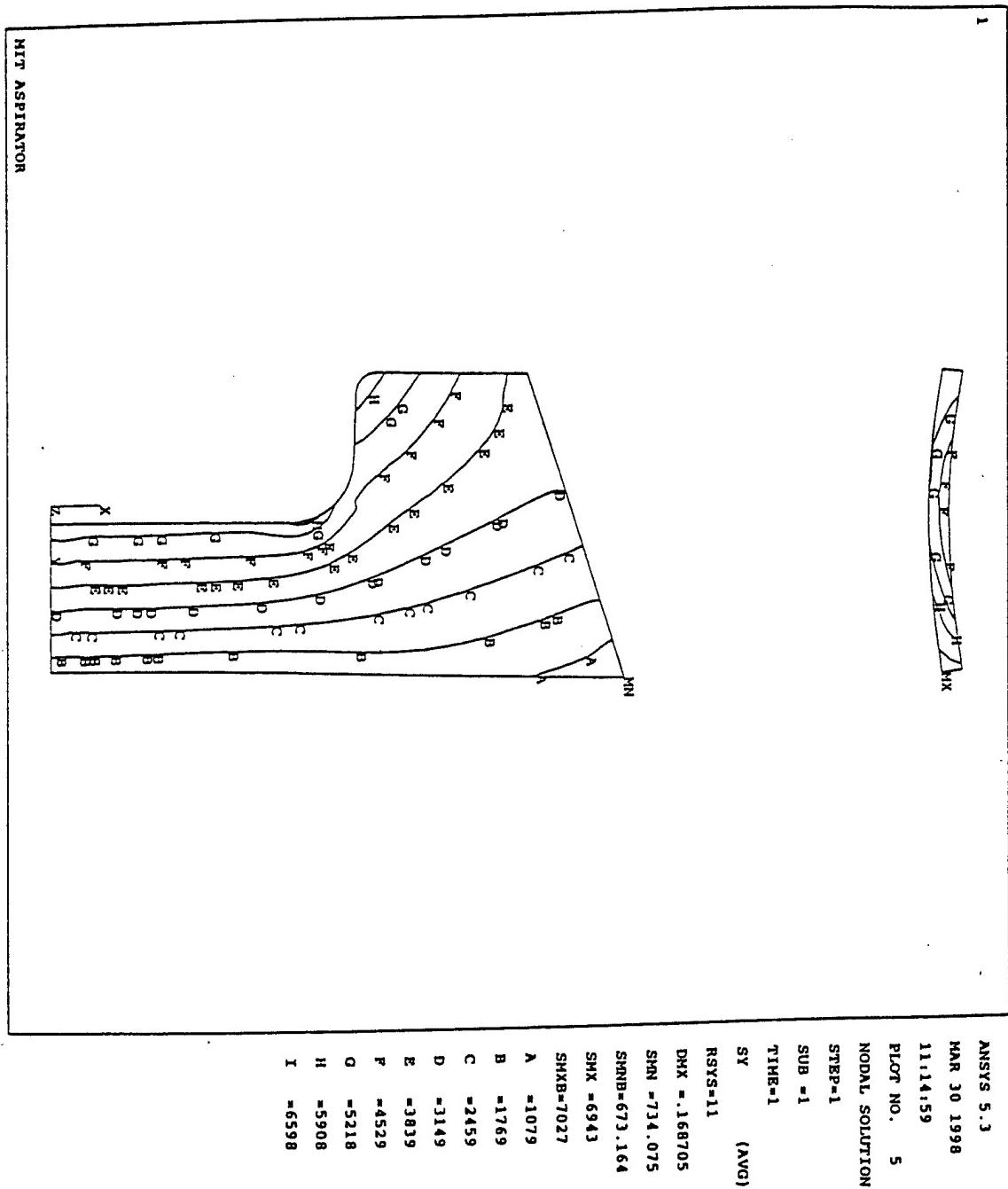
Figure A-6: Tangential Stress (psi)

49

The figure contains the following ANSYS plot legend text:

HIT ASPIRATOR

```
1
ANSYS 5.3
MAR 30 1998
11:15:01
PLOT NO.    6
NODAL SOLUTION
STEP=1
SUB =1
TIME=1
SZ        (AVG)
RSYS=11
DMX =.168705
SMN =-2165
SMNB=-2362
SMX =1611
SMXB=2119
A =-1955
B =-1535
C =-1116
D =-695.915
E =-276.167
F =143.582
G =563.331
H =983.08
I =1403
```
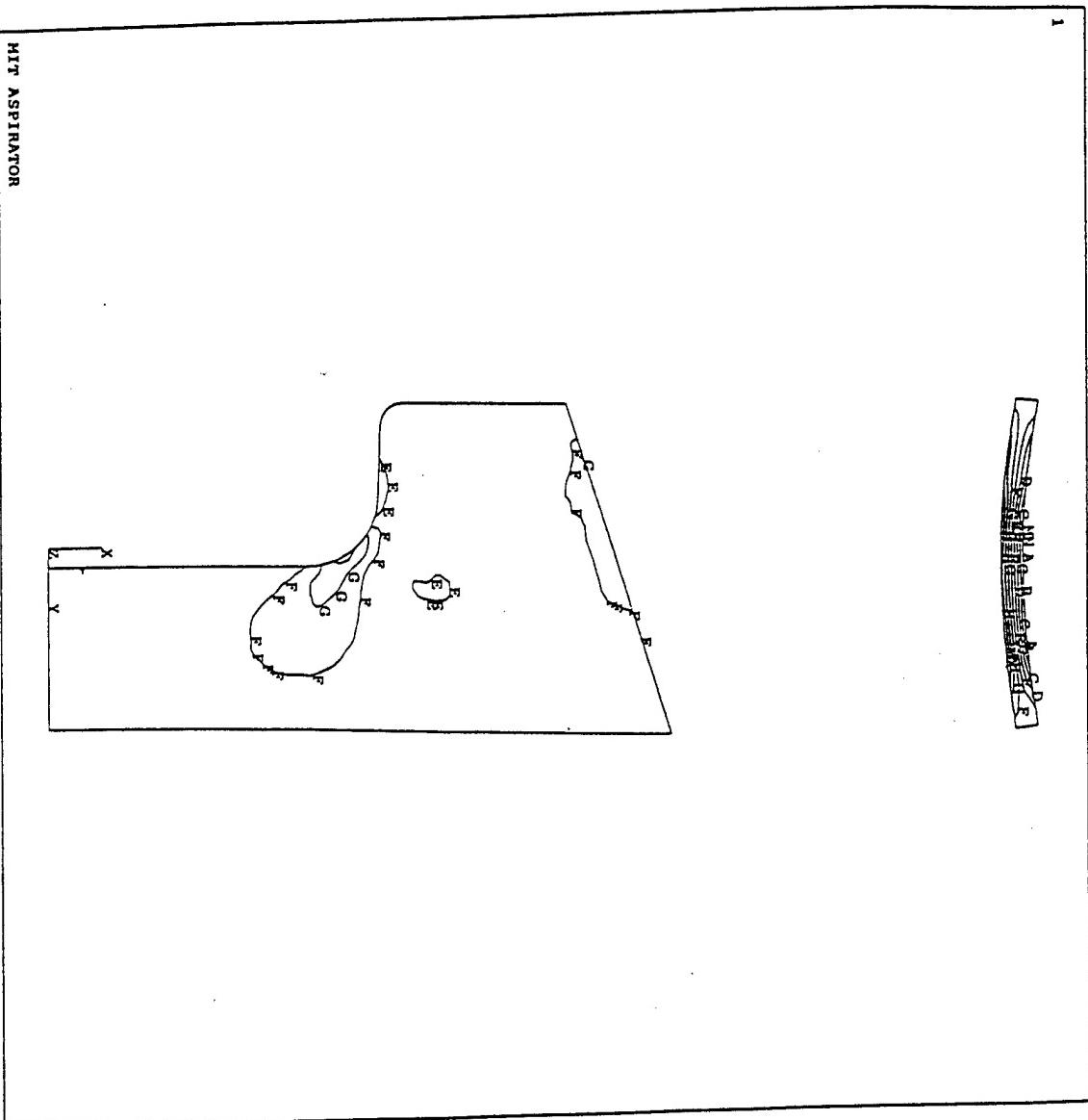
Figure A-7: Axial Stress (psi)

50
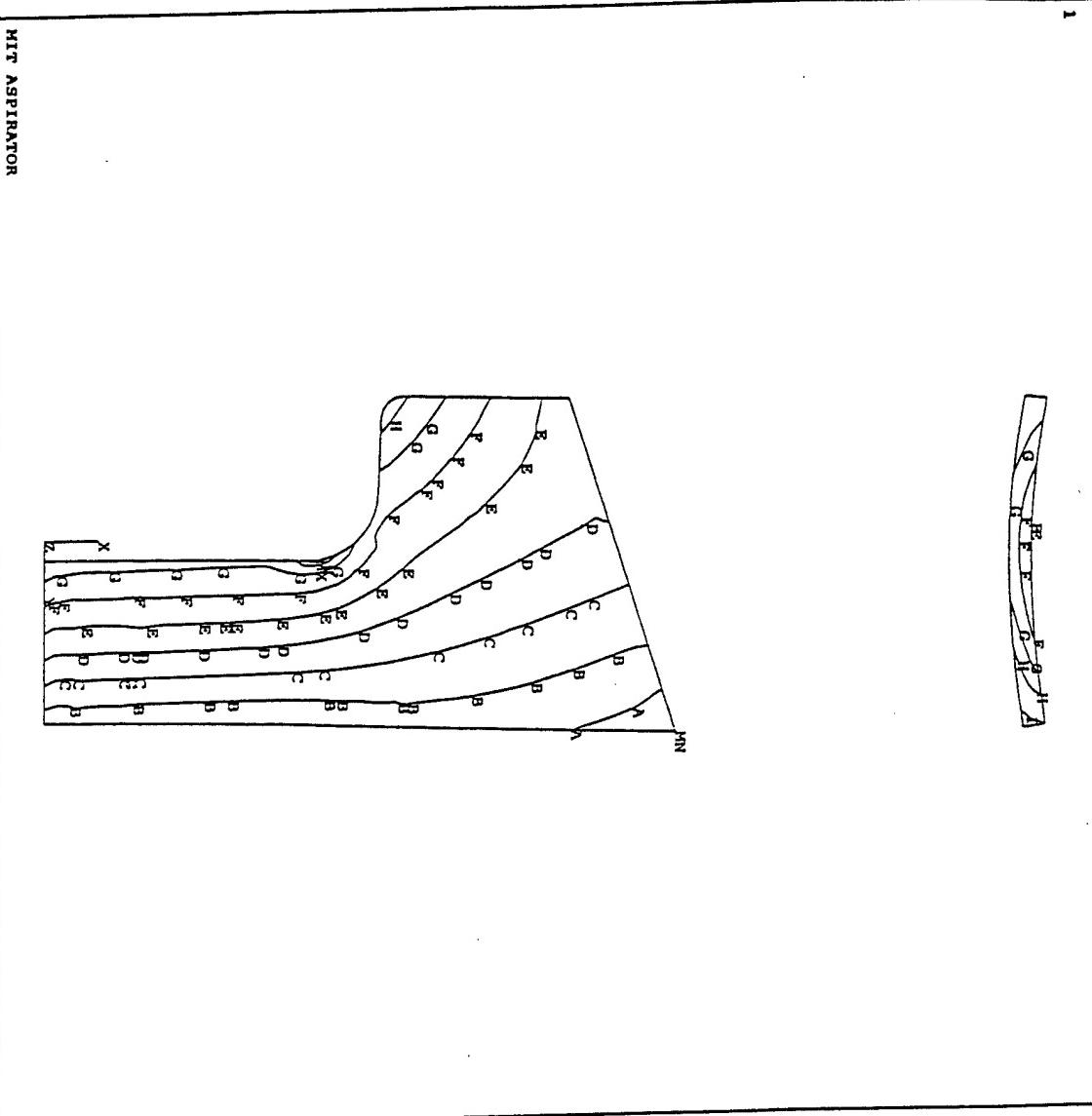
Figure A-8: Maximum Principle Stress (psi)

ANSYS 5.3
MAR 30 1998
11:15:04
PLOT NO.   8
NODAL SOLUTION
STEP=1
SUB =1
TIME=1
SEQV   (AVG)
DMX =.168705
SMN =702.755
SMNB=641.843
SMX =6947
SMXB=7031
A =1050
B =1743
C =2437
D =3131
E =3825
F =4519
G =5213
H =5906
I =6600
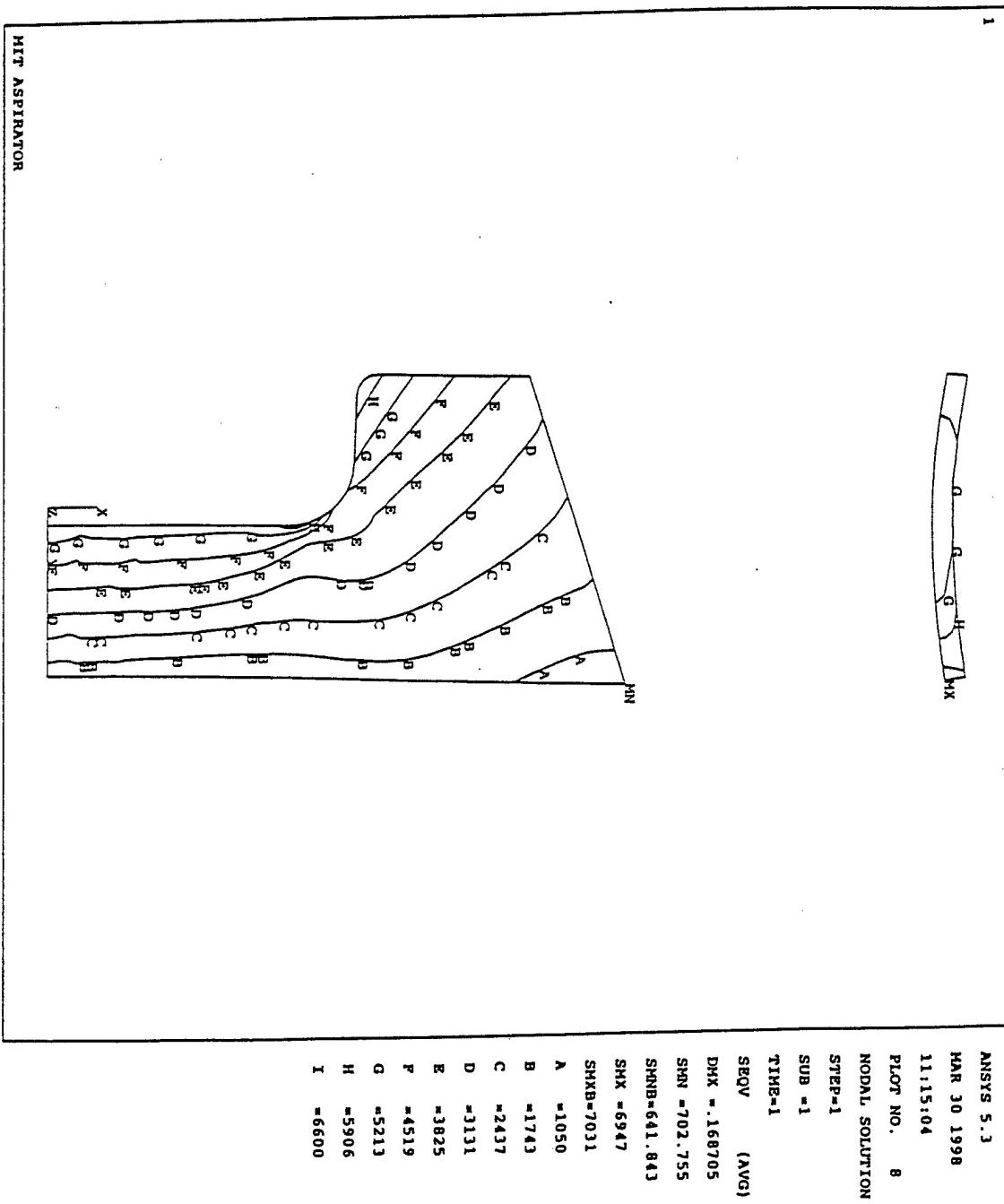
Figure A-9: Effective Stress (psi)

HIT ASPIRATOR

ANSYS 5.3
MAR 30 1998
11:15:26
PLOT NO.   9
NODAL SOLUTION
STEP=1
SUB =1
TIME=1
S1   (AVG)
DMX =.007805
SMN =1046
SMNB=-24306
SMX =40520
SMXB=70039

A =3239
B =7625
C =12011
D =16397
E =20783
F =25169
G =29555
H =33941
I =38327
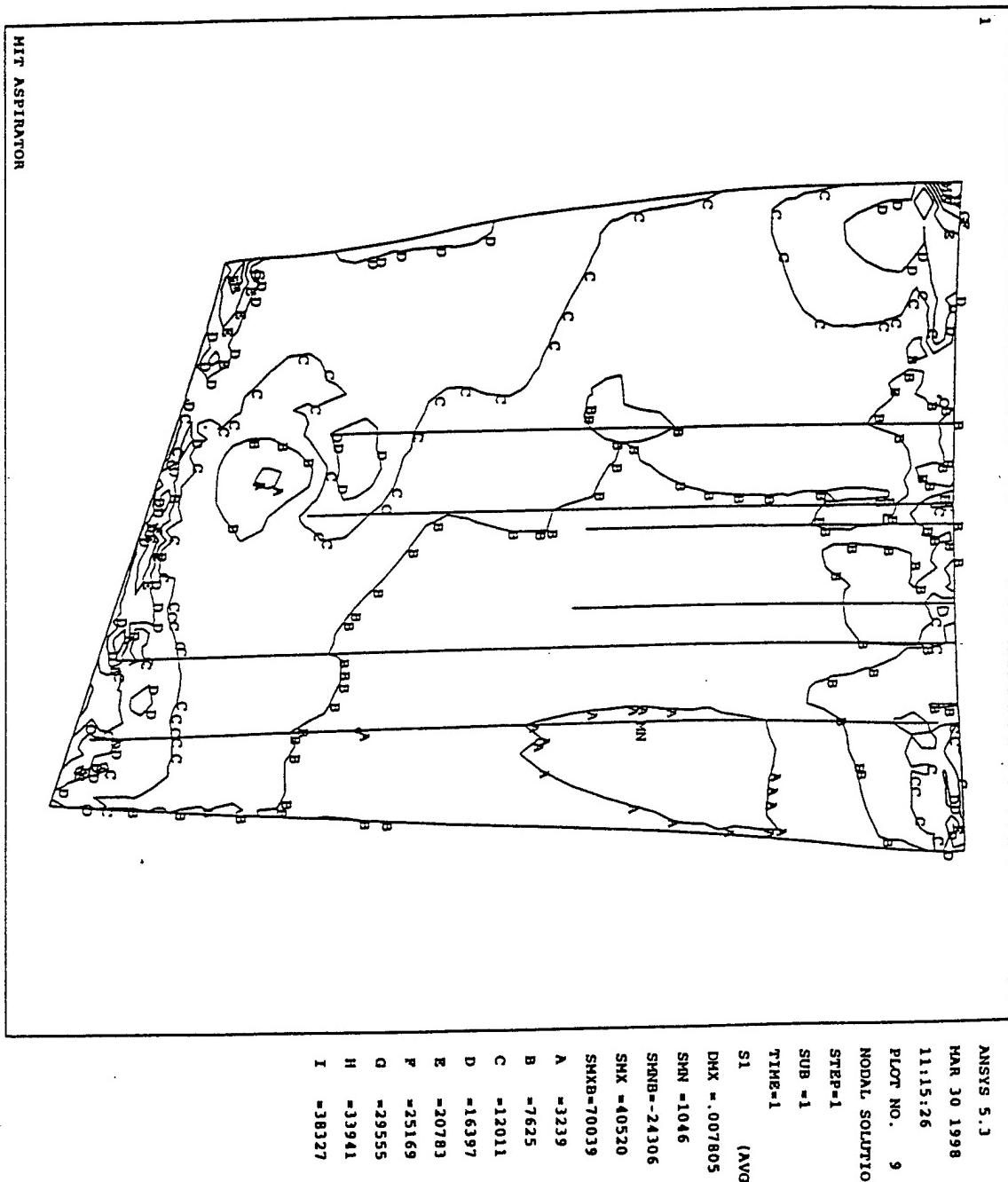
Figure A-10: Maximum Principle Stress on suction surface (psi)
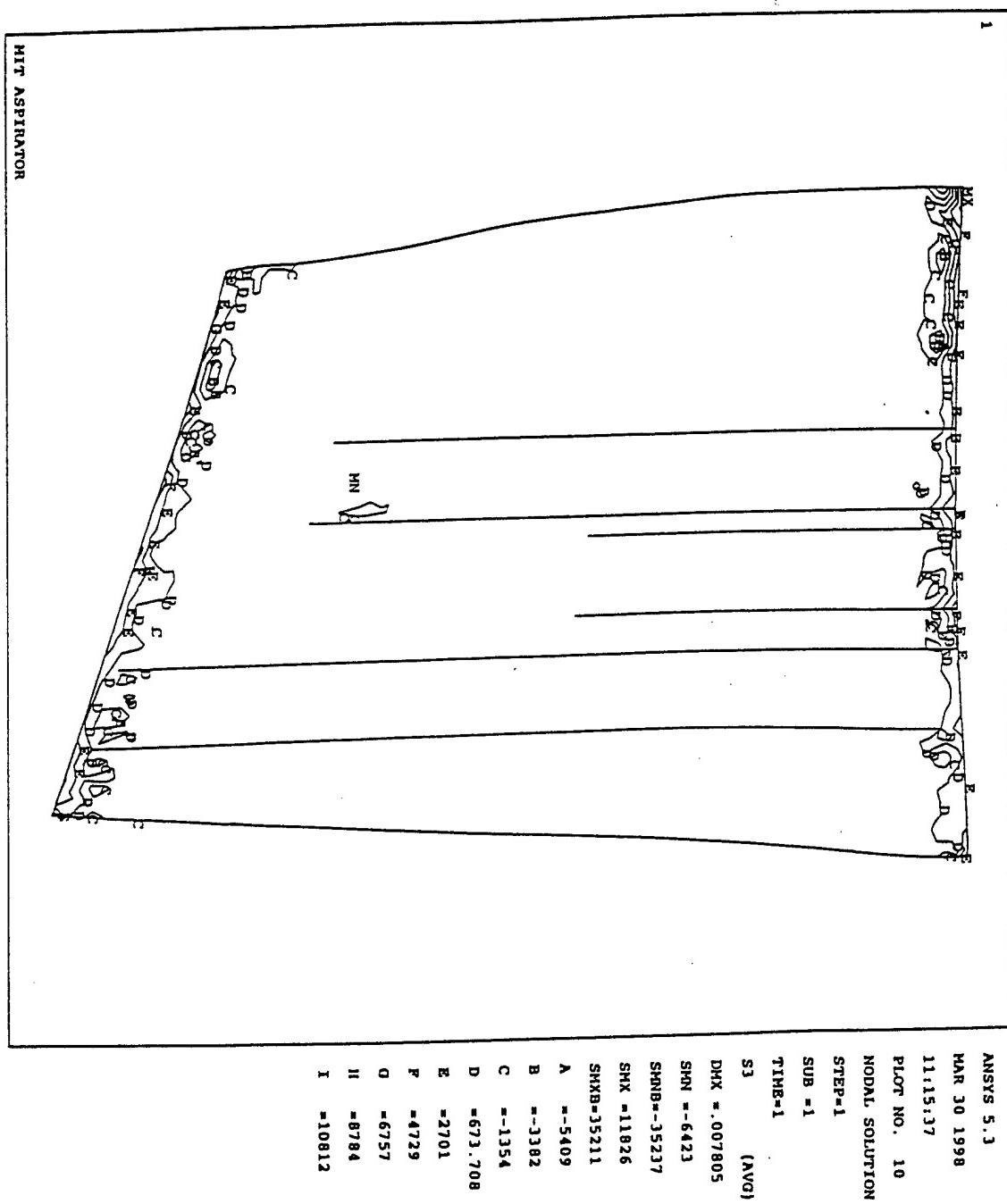
Figure A-11: Minimum Principle Stress on suction surface (psi)
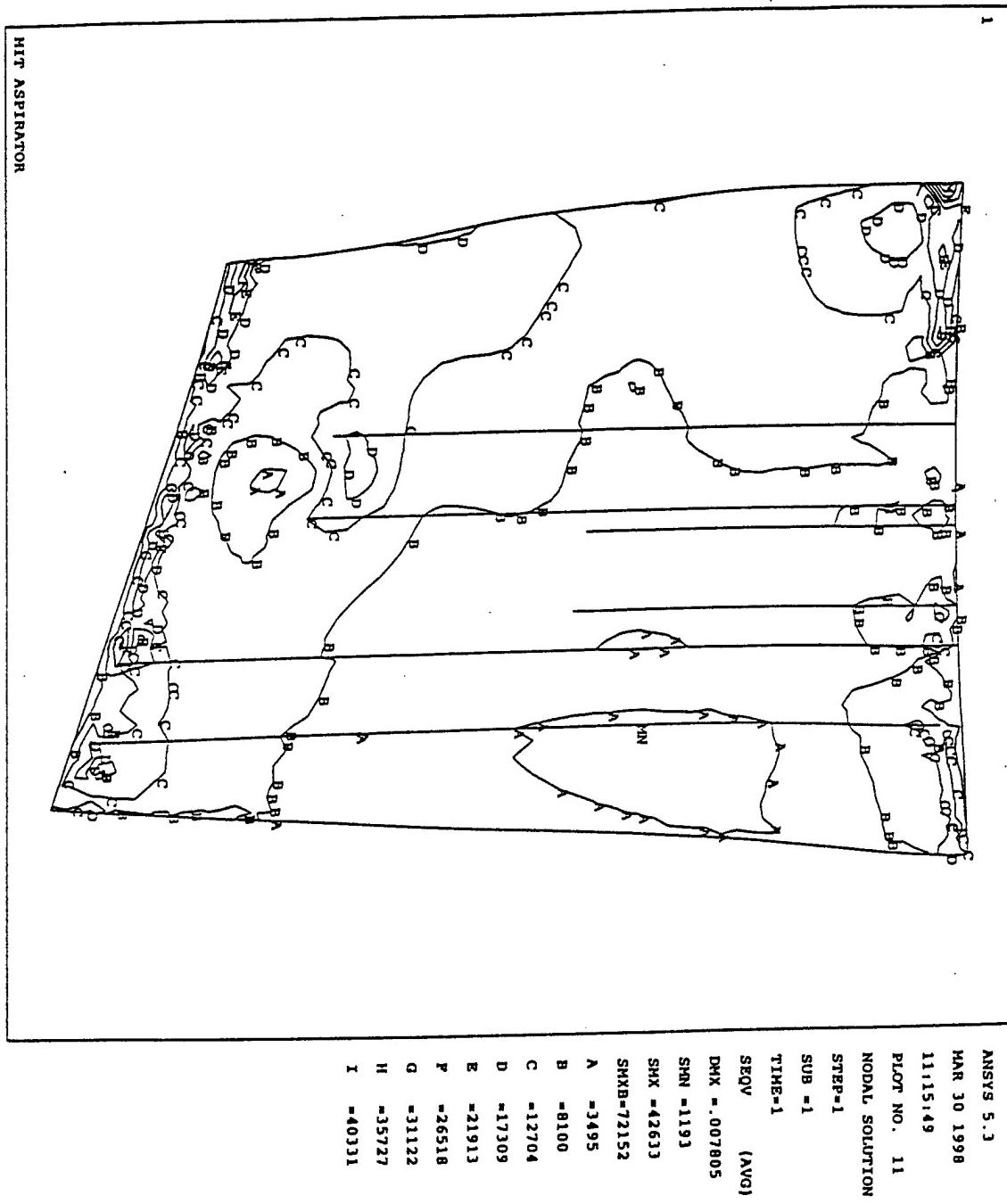
Figure A-12: Effective Stress on suction surface (psi)
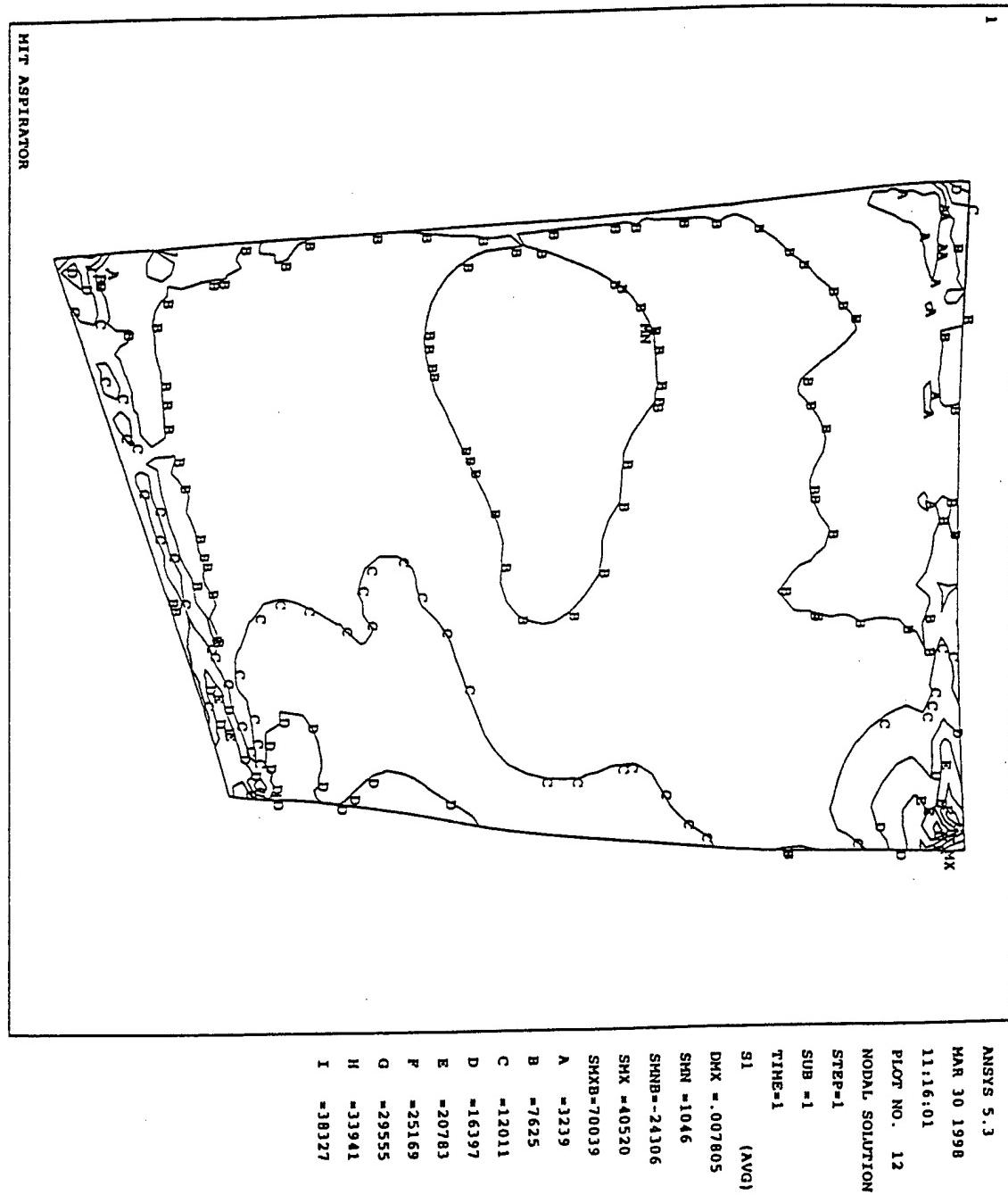
Figure A-13: Maximum Principle Stress on pressure surface (psi)
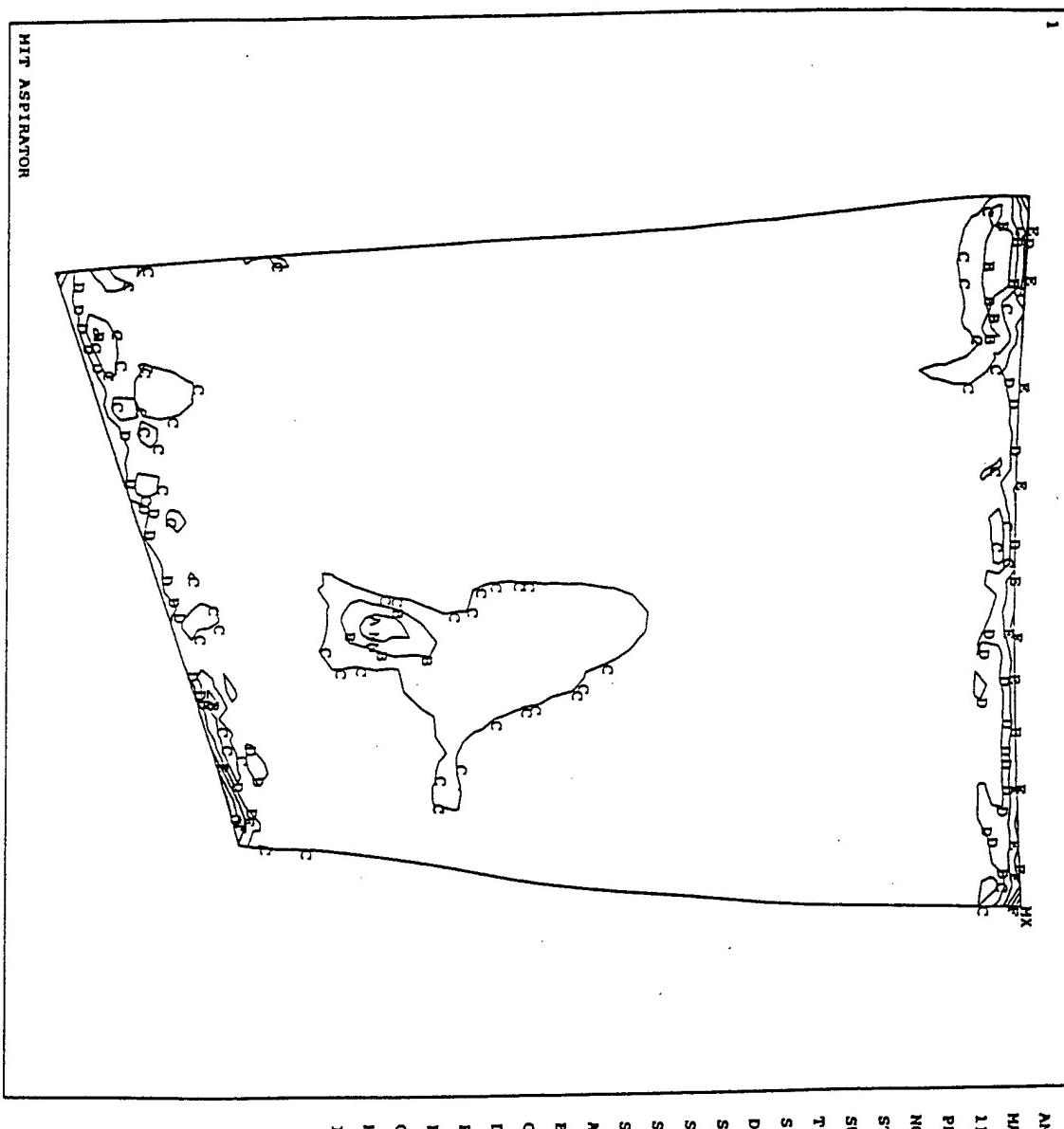
Figure A-14: Minimum Principle Stress on pressure surface (psi)

MIT ASPIRATOR

ANSYS 5.3
MAR 30 1998
11:16:23
PLOT NO. 14
NODAL SOLUTION
STEP=1
SUB =1
TIME=1
SEQV   (AVG)
DMX =.007805
SMN =1193
SMX =42633
SMXB=72152
A =3495
B =8100
C =12704
D =17309
E =21911
F =26518
G =31122
H =35727
I =40331
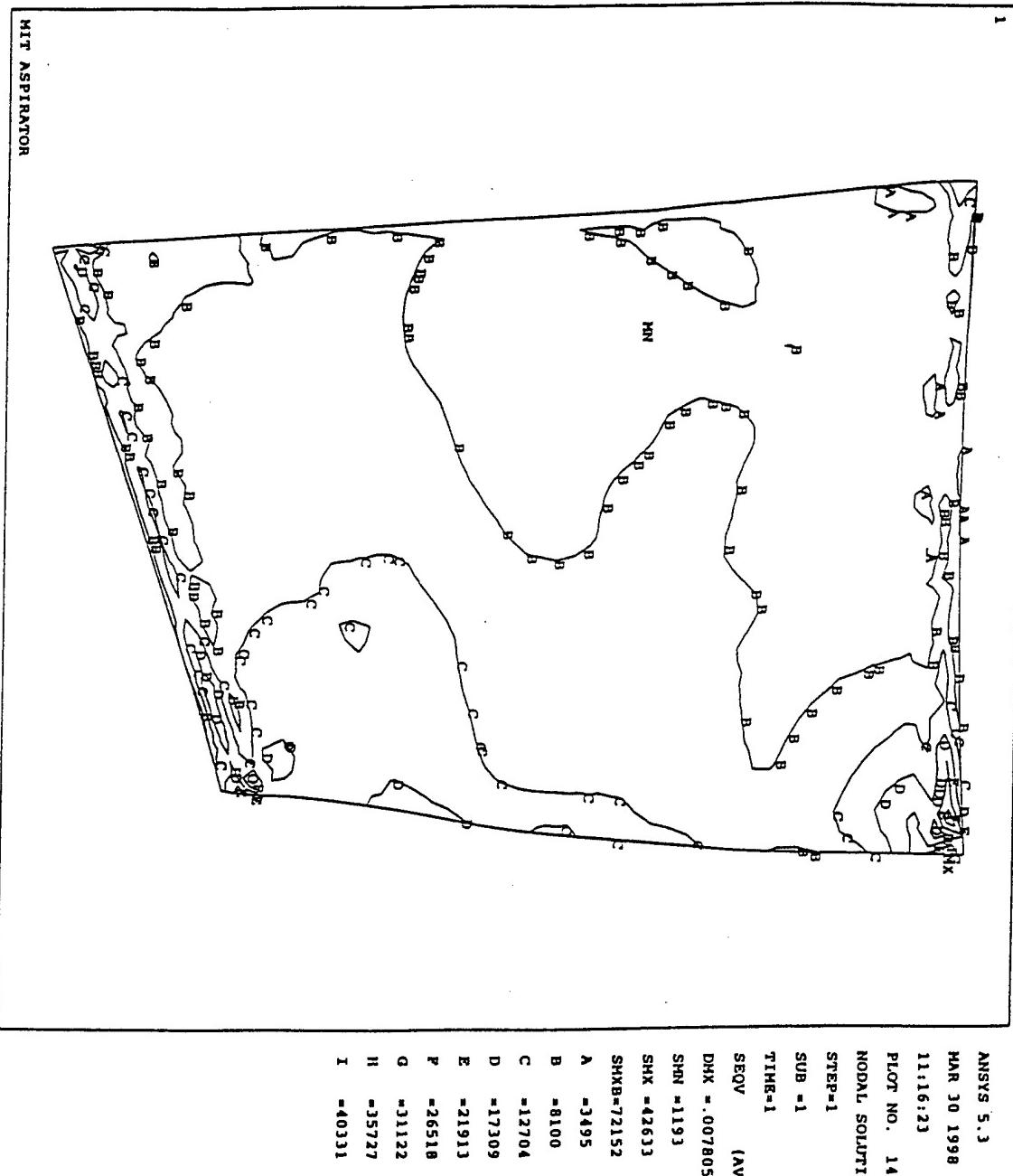
Figure A-15: Effective Stress on pressure surface (psi)

Appendix B

Engineering Drawings of Low Speed Aspirated Stage

This appendix contains the engineering drawings for the complete stage for implementation in the MIT Blowdown Compressor. An assembly drawing of the stage can be seen in the main text in figure 3-1.
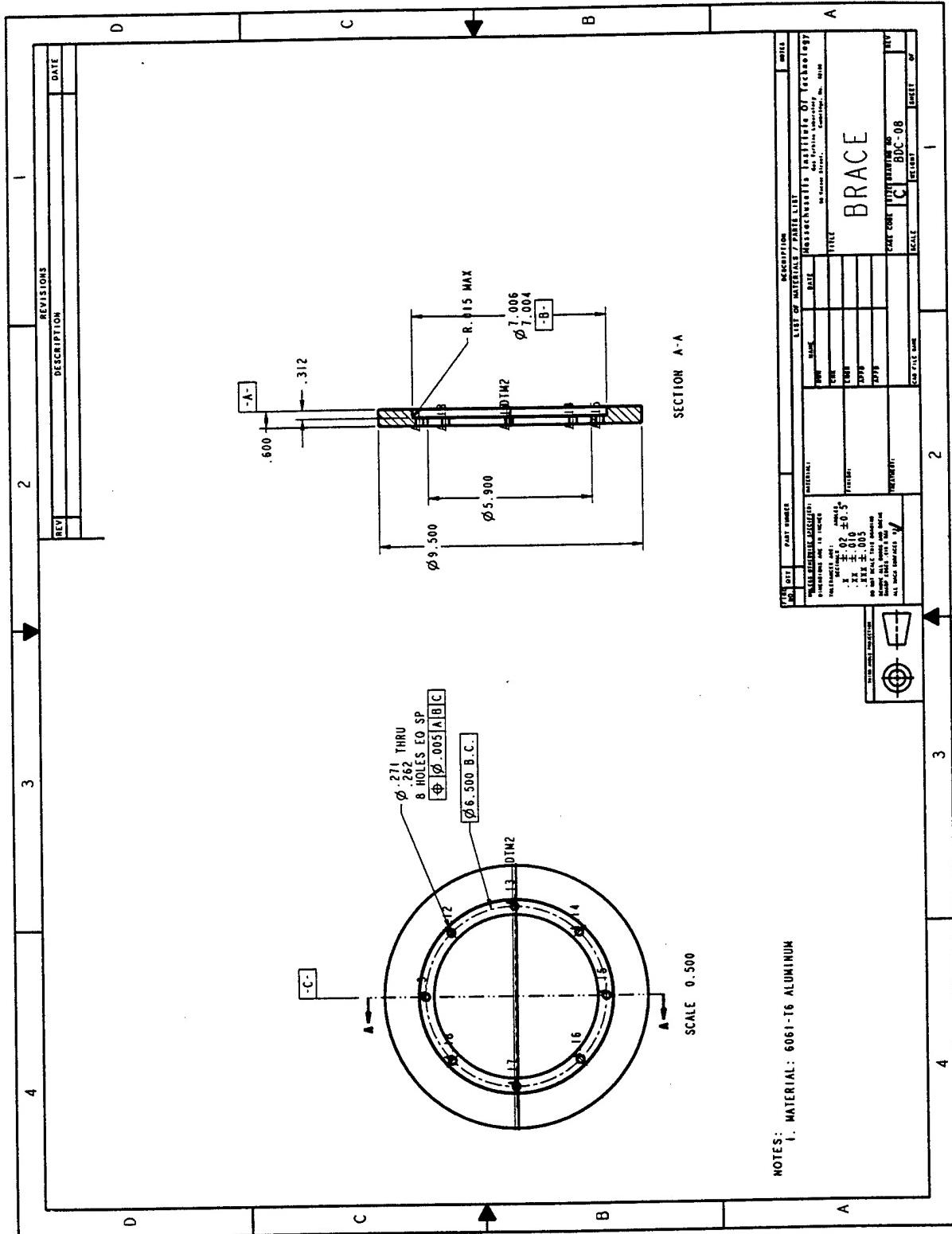
Figure B-1: Engineering drawing of the Brace
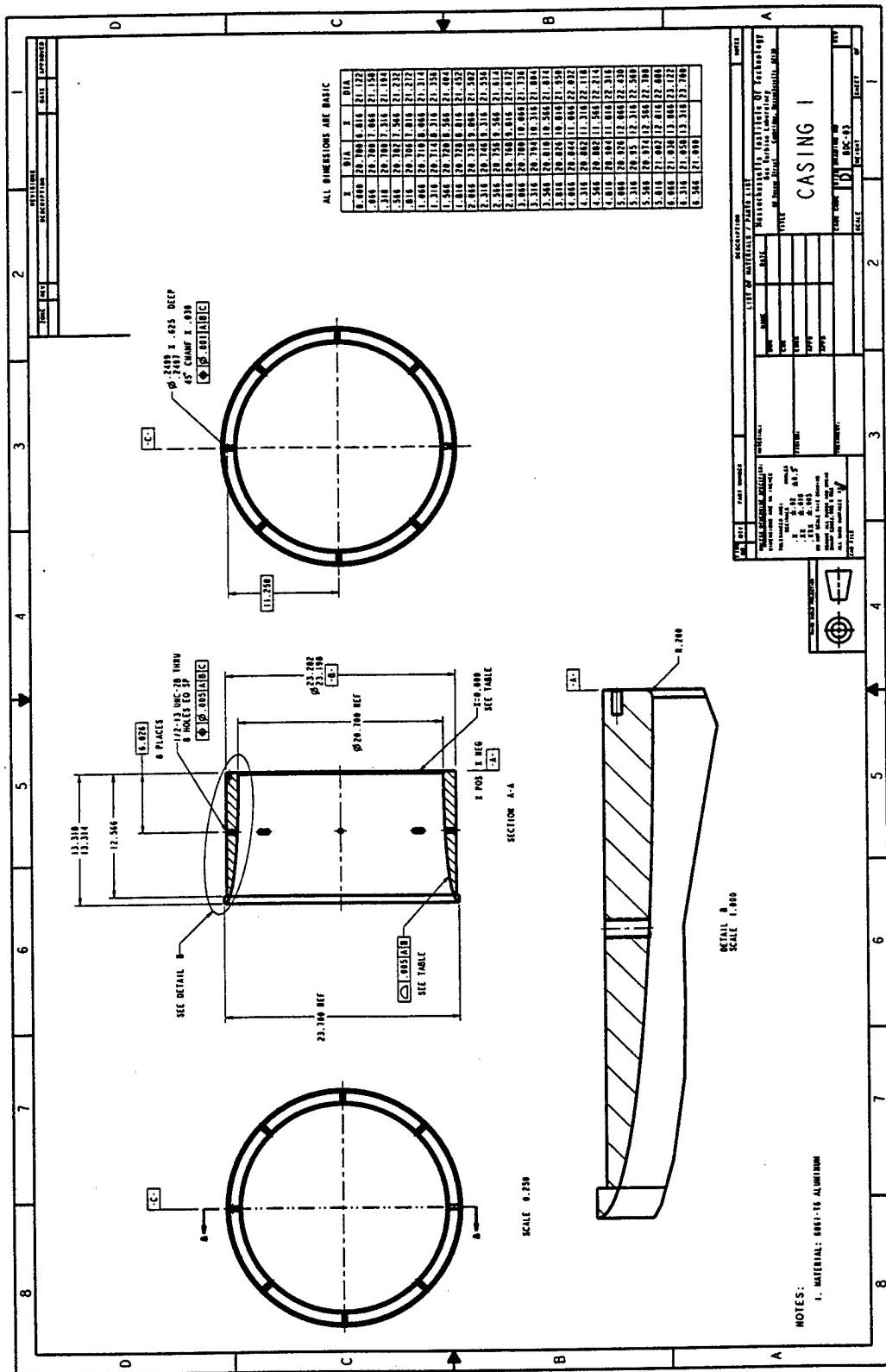
Figure B-2: Engineering drawing of the Casing 1
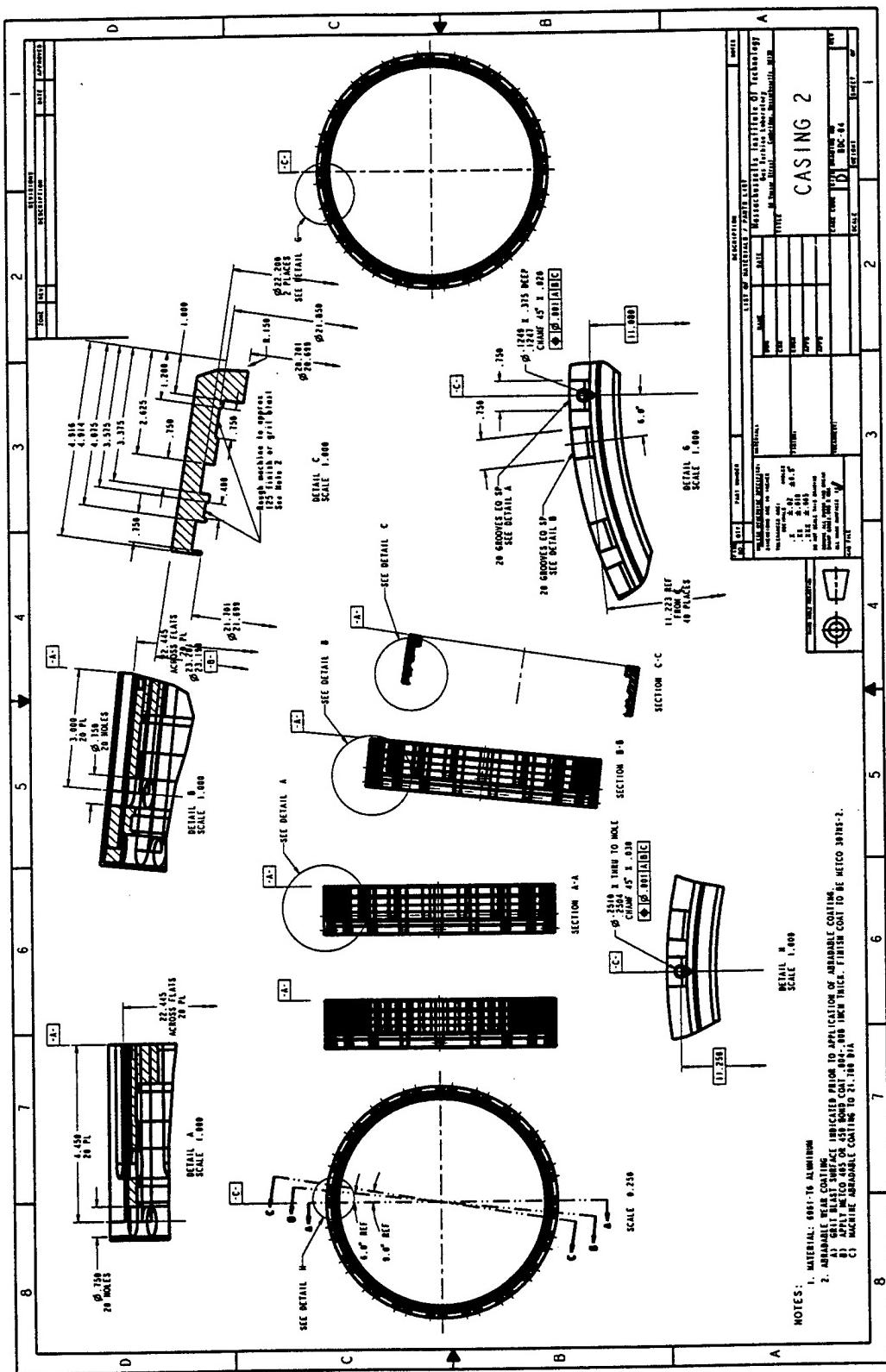
Figure B-3: Engineering drawing of the Casing 2

62
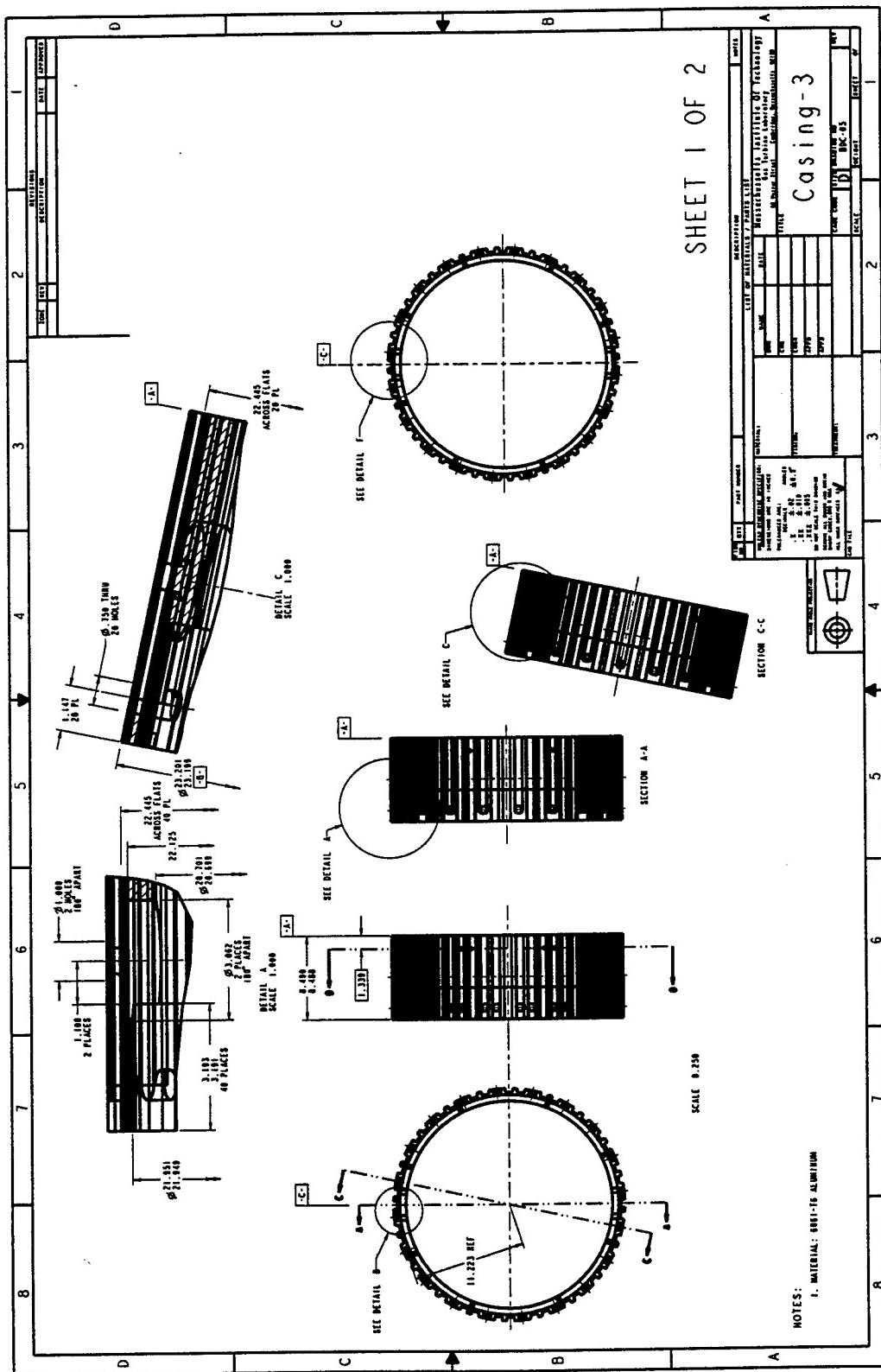
Figure B-4: Engineering drawing of sheet 1 of Casing 3

63
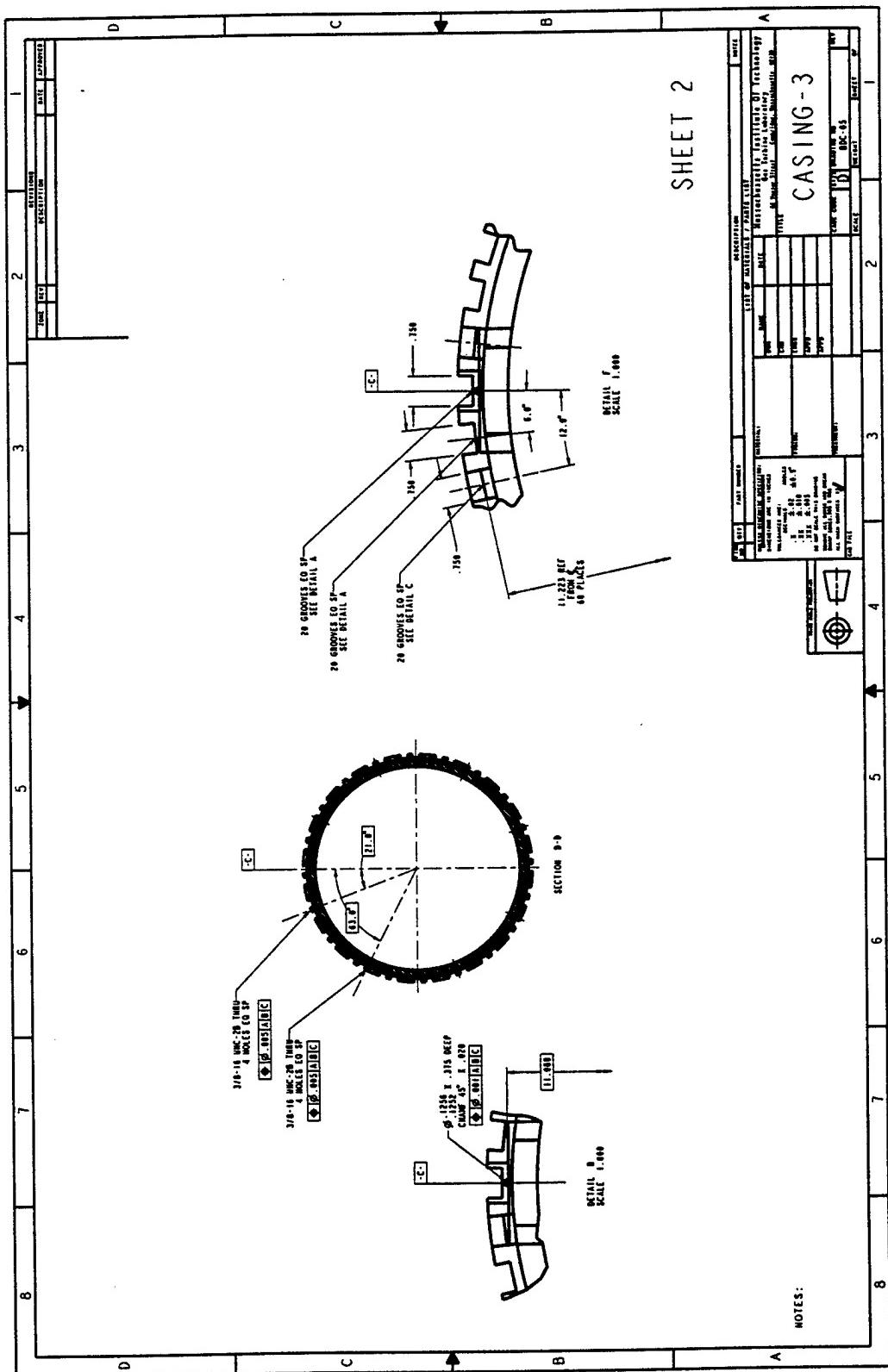
Figure B-5: Engineering drawing of sheet 2 of Casing 3
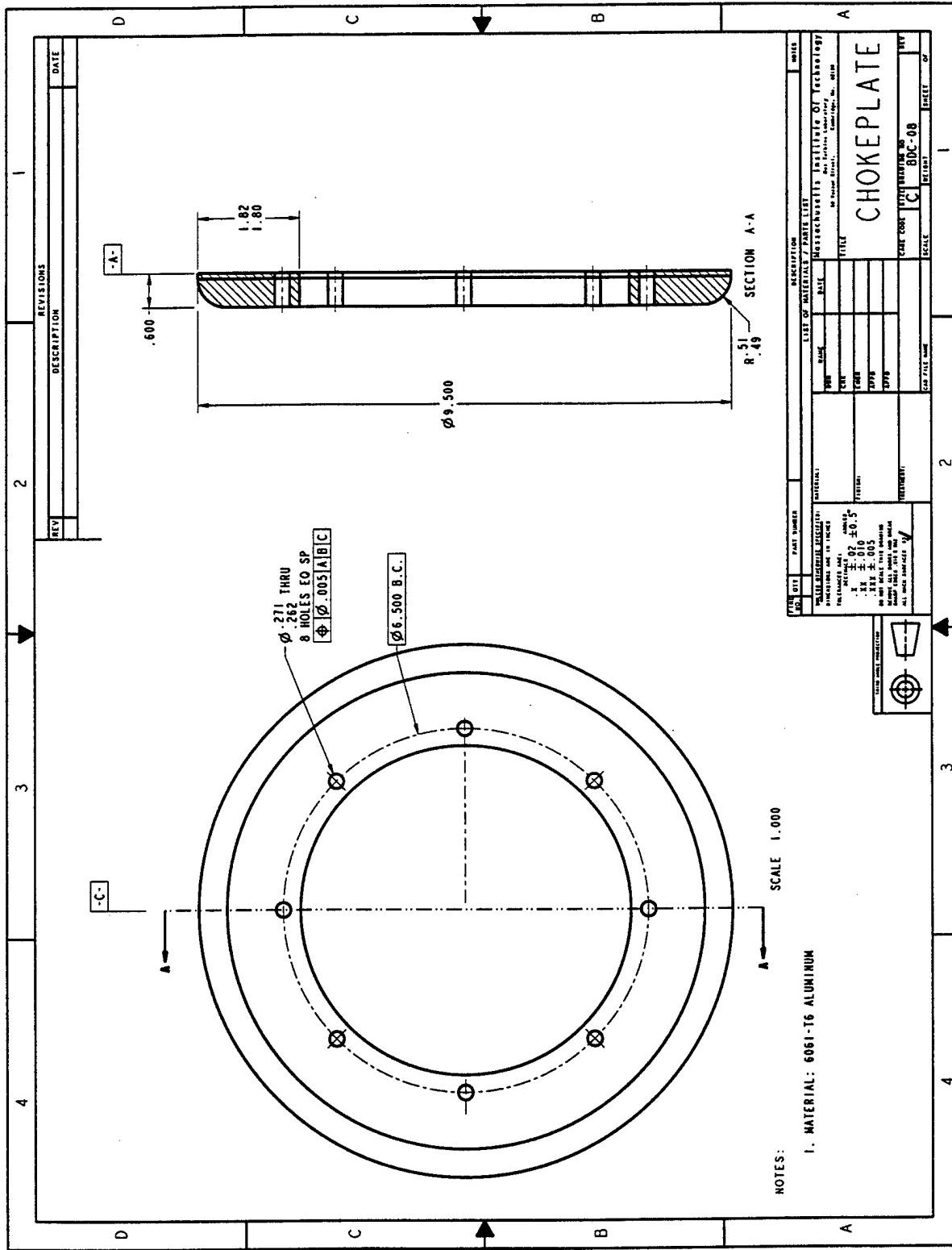
Figure B-6: Engineering drawing of the Chokeplate
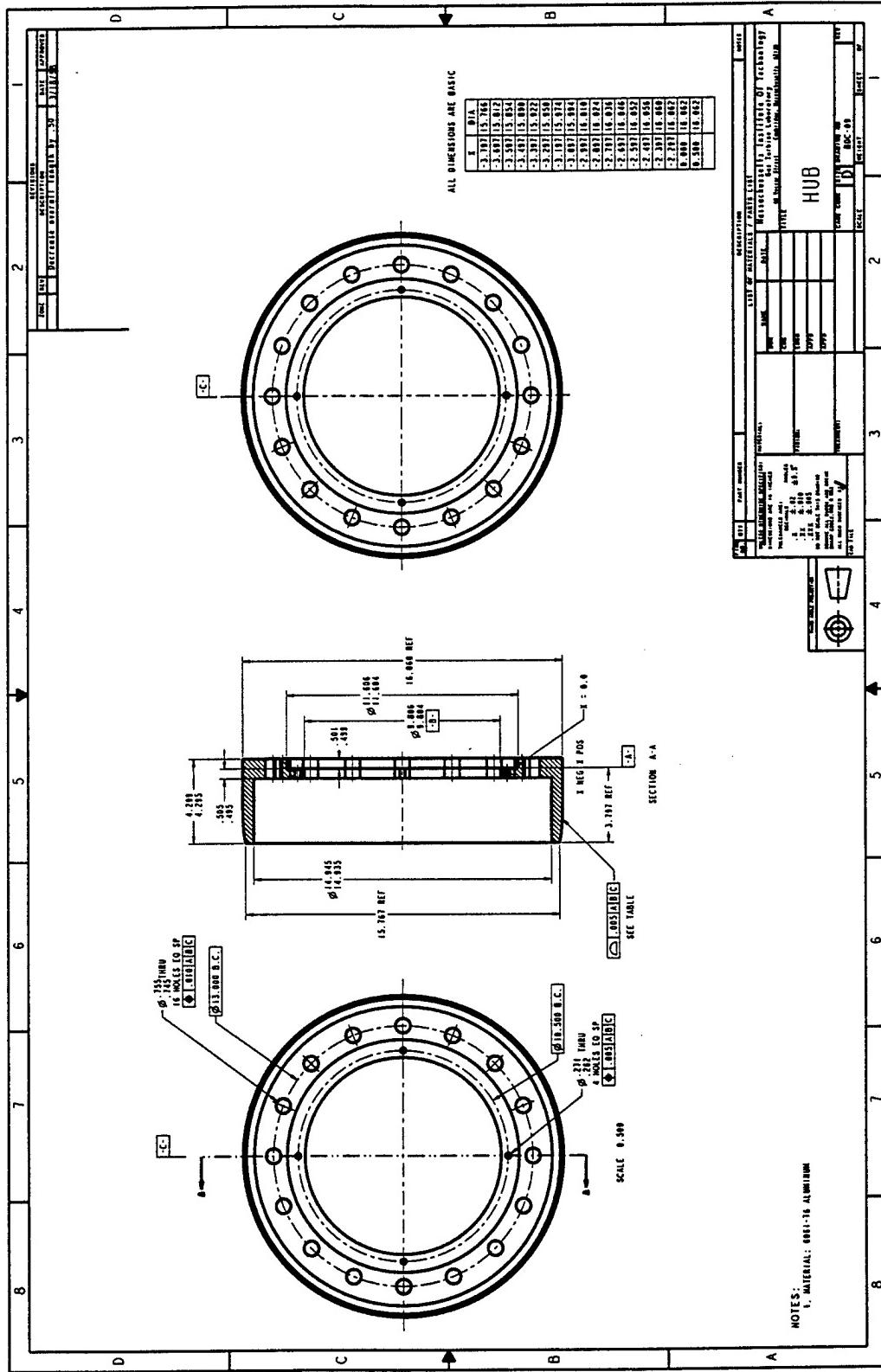
Figure B-7: Engineering drawing of the aft Hub

66
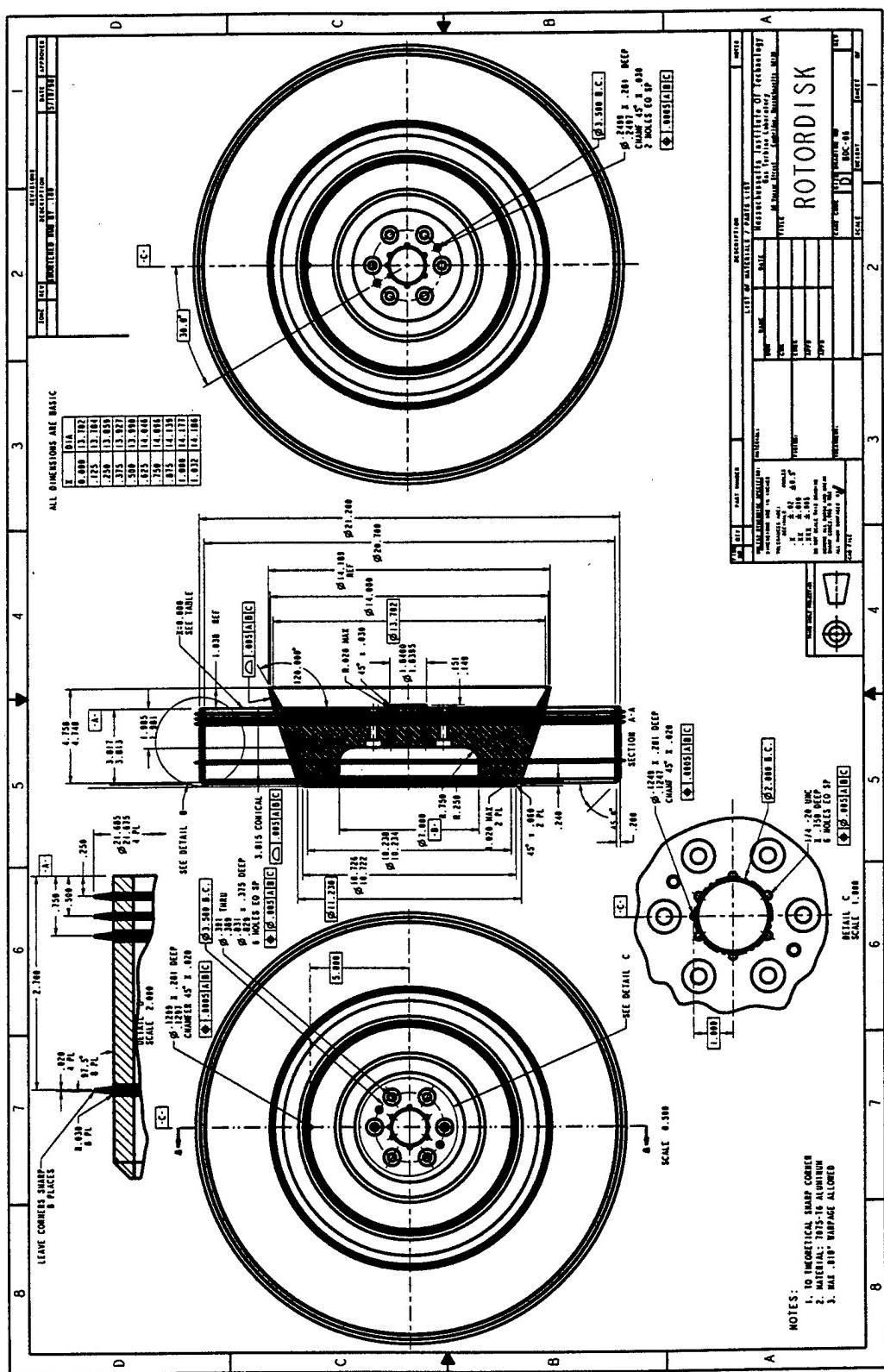
Figure B-8: Engineering drawing of the Rotordisk
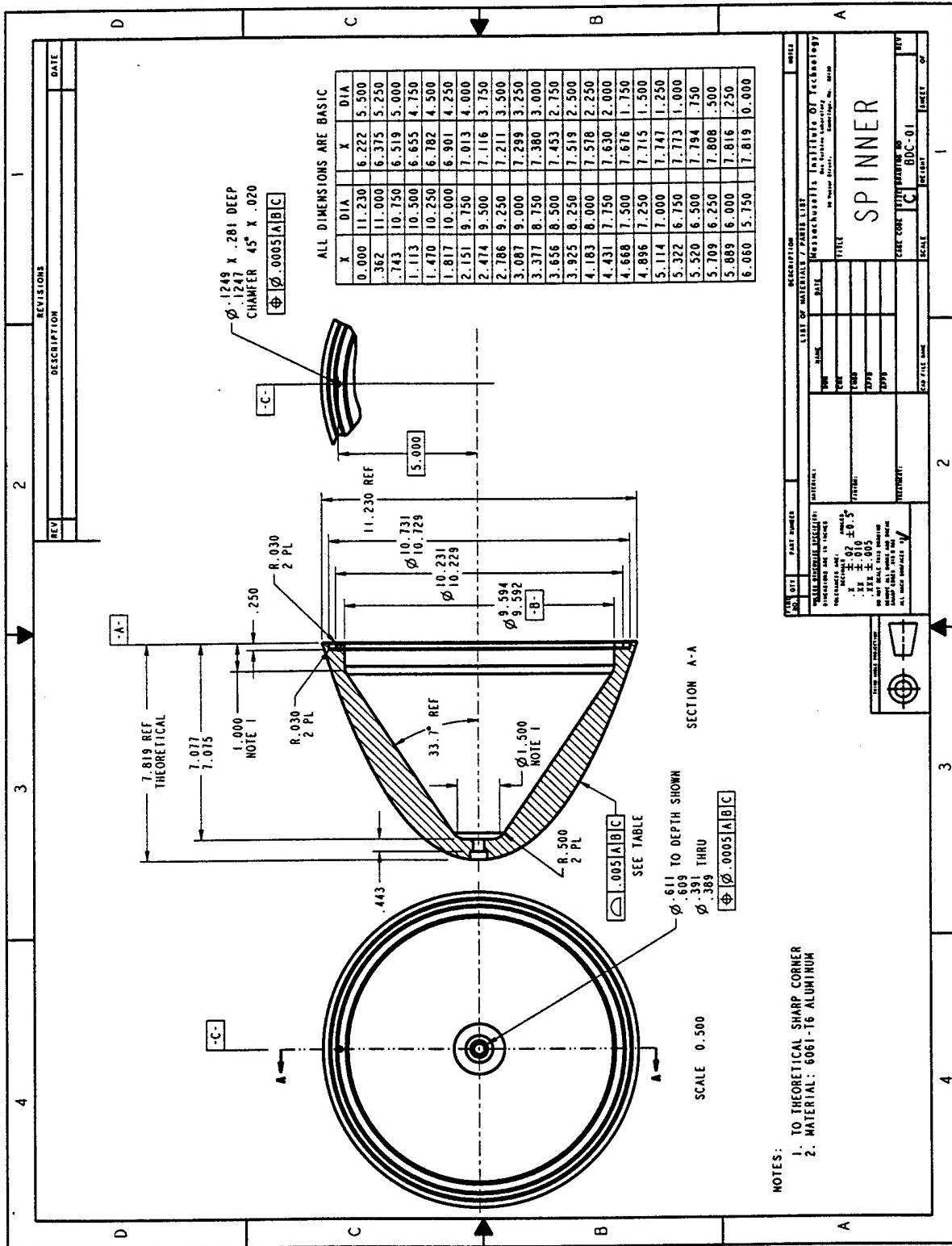
Figure B-9: Engineering drawing of the Spinner
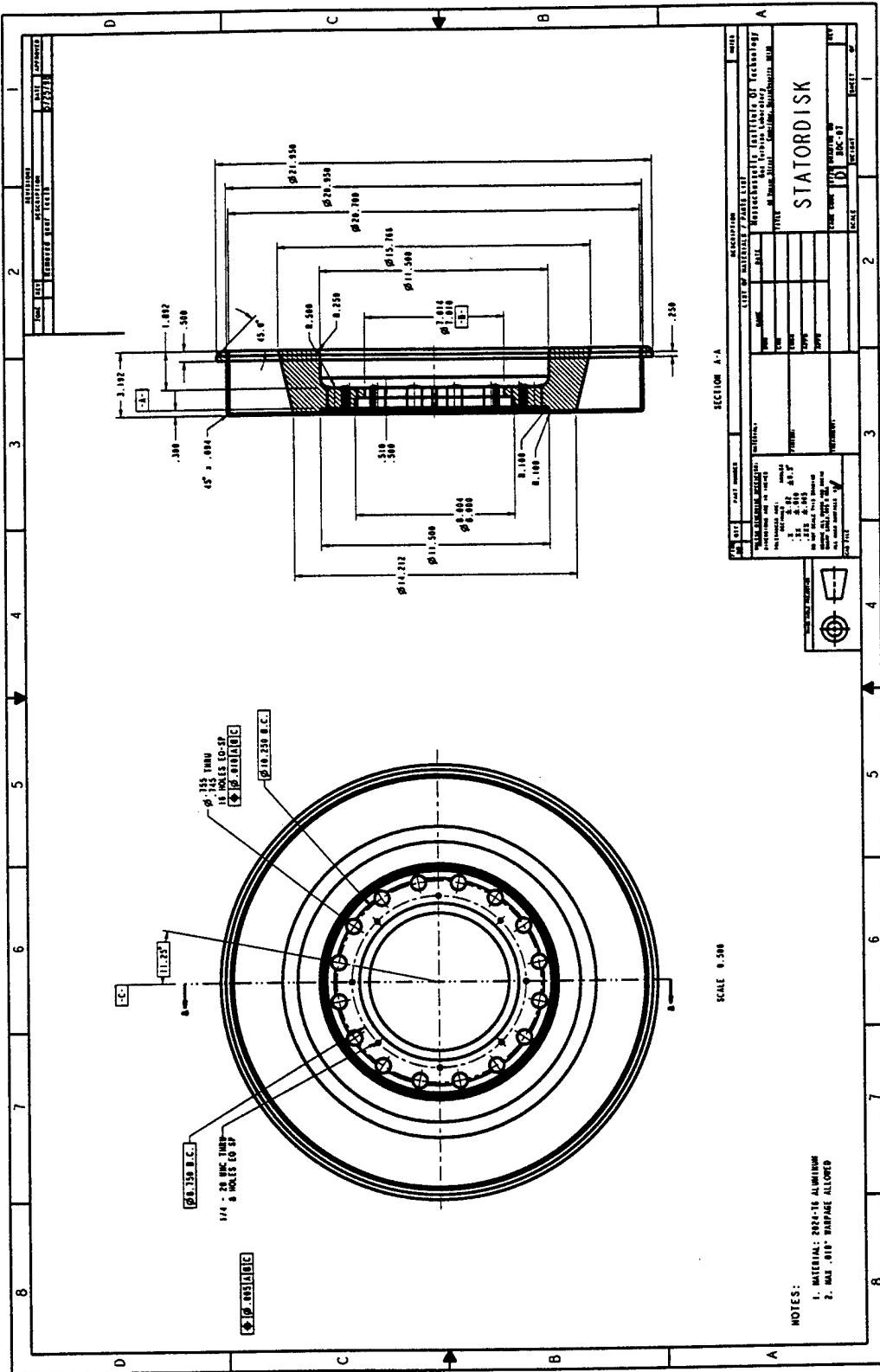
Figure B-10: Engineering drawing of the Statordisk
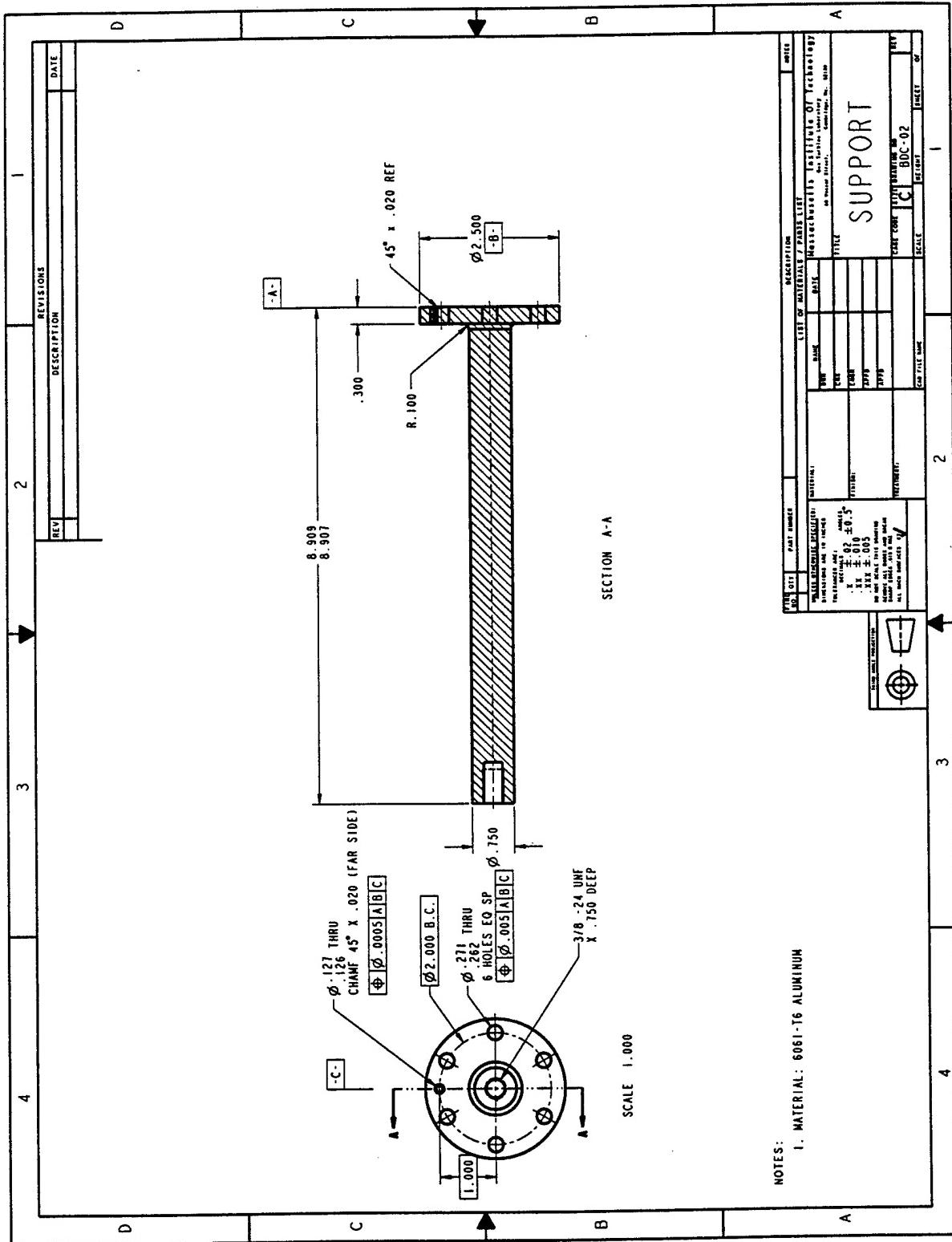
Figure B-11: Engineering drawing of the Support

Bibliography

[1] J. L. Kerrebrock, M. Drela, A. A. Merchant, and B. J. Schuler. A Family of Designs for Aspirated Compressors. In *ASME Turbomachinery Conference*, 1998.

[2] J. L. Kerrebrock, D. P. Reijnen, W. S. Ziminsky, L. M. Smilg, and J. E. Dennis. Aspirated Compressors. In *ASME Turbomachinery Conference*, 1997.

[3] Jack L. Kerrebrock. The M.I.T. Blowdown Compressor Facility. Technical Report 108, M.I.T. Gas Turbine Lab, May 1972.

[4] Ali. A. Merchant. Design and Analysis of Supercritical Airfoils with Boundary Layer Suction. Master's thesis, Massachusetts Institute of Technology, 1996.

[5] Duncan P. Reijnen. *Experimental Study of Boundary Layer Suction in a Transonic Compressor*. PhD thesis, Massachusetts Institute of Technology, January 1997.